AGU PUBLICATIONS

JGR

Journal of Geophysical Research: Oceans

RESEARCH ARTICLE

10.1002/2013JC009511

Key Points:
- Analyses of a 106 year record of fast-ice from the Southern Ocean
- Timings of formation and breakout are affected by different processes
- Frequencies of variability change with no trend over last 30 years

Correspondence to:
E. J. Murphy,
e.murphy@bas.ac.uk

Citation:
Murphy, E. J., A. Clarke, N. J. Abram, and J. Turner (2014), Variability of sea-ice in the northern Weddell Sea during the 20th century, *J. Geophys. Res. Oceans*, *119*, 4549–4572, doi:10.1002/2013JC009511.

Received 21 OCT 2013
Accepted 2 JUL 2014
Accepted article online 5 JUL 2014
Published online 28 JUL 2014

Variability of sea-ice in the northern Weddell Sea during the 20th century

E. J. Murphy[1], A. Clarke[1,2], N. J. Abram[1,3], and J. Turner[1]

[1]British Antarctic Survey, NERC, Cambridge, UK, [2]School of Environmental Sciences, University of East Anglia, Norwich, UK, [3]Research School of Earth Sciences, Australian National University, Canberra, ACT, Australia

Abstract The record of winter fast-ice in the South Orkney Islands, northern Weddell Sea, Antarctica, is over a century long and provides the longest observational record of sea-ice variability in the Southern Hemisphere. Here we present analyses of the series of fast-ice formation and breakout dates from 1903 to 2008. We show that over the satellite era (post-1979), the timing of both final autumn formation and complete spring breakout of fast-ice is representative of the regional sea-ice concentrations (SIC) in the northern Weddell Sea, and associated with atmospheric conditions in the Amundsen Sea region to the west of the Antarctic Peninsula. Variation in the fast-ice breakout date is influenced by the intensity of the westerly/north-westerly winds associated with the Southern Annular Mode (SAM). In contrast, the date of ice formation displays correlations with regional oceanic and sea-ice conditions over the previous 18 months, which indicate a preconditioning during the previous summer and winter, and exhibits variability associated with variation in tropical Pacific sea-surface temperature (i.e., the El Niño-Southern Oscillation, ENSO). A reduction in fast-ice duration at the South Orkney Islands around the 1950s was associated with both later formation and earlier breakout. However, there were marked changes in variability (with periodicities of 3–5, 7–9, and 20 years) in each of the series and in their relationships with ENSO and SAM, indicating the need for caution in interpreting changes in ice conditions based on shorter-term satellite series.

1. Introduction

Sea-ice is a major component of the climate system, influencing globally important atmospheric and oceanic processes throughout the polar regions [*Turner and Overland*, 2009]. Sea-ice also influences the structure and functioning of polar marine ecosystems, affecting biogeochemical cycles, the life cycles of many species and their interactions within food webs [*Brierley and Thomas*, 2002; *Nicol et al.*, 2008]. In the Antarctic, changes in sea-ice extent (SIE) over the last few decades have been associated with regional fluctuations in atmospheric conditions [*Turner and Overland*, 2009]. These changes in the concentration, distribution, and seasonality of sea-ice have had major impacts on biological systems, affecting every trophic level in ecosystems throughout the Southern Ocean [*Clarke et al.*, 2007; *Ducklow et al.*, 2007; *Murphy et al.*, 2007b; *Melbourne-Thomas et al.*, 2013]. Interannual variability is a significant feature of regional sea-ice cover and can obscure any longer term (>10 years) changes [*Stammerjohn et al.*, 2008a, 2008b; *Yuan and Li*, 2008; *Kravchenko et al.*, 2011]. There is a clear need to understand whether particular patterns of interannual and subdecadal variability are the result of natural intrinsic variations in the physical environment or whether they reflect a more systematic change in the climate system. This type of assessment can only be made with a sufficiently long record of past sea-ice changes, but such data are almost entirely lacking for the Southern Ocean.

Satellite data show that sea-ice around Antarctica has undergone a small, but significant, increase in circumpolar SIE of 0.97% decade^{-1} for the period from 1978 to 2007 [*Turner and Overland*, 2009]. There is, however, marked regional variation, with a negative trend in SIE in the Amundsen-Bellingshausen Sea (ABS) (−6.63% decade^{-1}) and a positive trend in the Ross Sea region [4.43% decade^{-1}; see also *Yuan and Martinson*, 2000; *Zwally et al.*, 2002; *Comiso and Nishio*, 2008]. The factors generating regional sea-ice variability around Antarctica have been previously examined using the relatively short satellite-based records, and interactions have been identified with patterns of atmospheric circulation, which affect temperature, wind speed, and wind direction and advection.

The major modes of climate variability affecting the Antarctic are the Southern Annular Mode (SAM) and the tropical El Niño-Southern Oscillation (ENSO) [see, e.g., *Pezza et al.*, 2008, 2012; *Stammerjohn et al.*, 2008b;

Yuan and Li, 2008; *Marshall et al*., 2011]. The SAM is the leading mode of extratropical climate variability in the Southern Hemisphere [*Thompson and Wallace*, 2000]. It is characterized by the large-scale alternation of atmospheric mass between a node centered over Antarctica and an annulus over the midlatitude Southern Ocean. It is also associated with a meridional shift in the intensity of the circumpolar westerly winds [*Hartmann and Lo*, 1998], which in turn influence northerly ice transport. Variations in the tropical El Niño-Southern Oscillation phenomenon (ENSO) also impact the Southern Ocean through low-to-high latitude teleconnections that are now reasonably well established [*Yuan and Martinson*, 2000; *Turner*, 2004; *Holland and Raphael*, 2006; *Lefebvre and Goosse*, 2008; *Meredith et al*., 2008; *Yuan and Li*, 2008]. Teleconnections associated with ENSO variability in the tropical Pacific have their strongest Southern Ocean impact in the ABS sector [*Turner*, 2004; *Turner et al*., 2013]. The variability creates anomalous high- (low-) pressure anomalies in the ABS in response to ENSO warm (cold) events [*Turner et al*., 2012, 2013]. The pressure system in the region, known as the Amundsen Sea Low (ASL), generates out-of-phase sea-ice/temperature anomalies east of the Ross Sea and in the Weddell Sea through both thermodynamic and dynamic processes. This pattern of variability is also termed the Antarctic Dipole [*Liu et al*., 2004; *Hobbs and Raphael*, 2010; *Wu and Zhang*, 2011; *Turner et al*., 2013].

Although associated with different physical processes, the ENSO and SAM climate modes interact as part of the southern high-latitude climate system to reinforce or dampen oceanic and sea-ice anomalies, which may also propagate spatially through oceanic or wind driven advection [*Murphy et al*., 1995; *Holland and Raphael*, 2006; *Meredith et al*., 2008; *Stammerjohn et al*., 2008b; *Yuan and Li*, 2008; *Wu and Zhang*, 2011; *Holland and Kwok*, 2012]. Using satellite data on sea-ice distribution, *Stammerjohn et al*. [2008b] have shown how atmospheric circulation patterns associated with different phases of SAM and ENSO affect the timing of regional sea-ice advance and retreat. There remain, however, significant questions about how these interactive effects are modified in different regions of the Southern Ocean and whether the relationships between processes are stable on decadal and longer time scales.

Only limited data are available on Antarctic sea-ice prior to the satellite era. These include ship observations and whale catch locations, station-based records of winter fast-ice, and proxy estimates based on records of the chemical composition of ice cores [*Murphy et al*., 1995; *de La Mare et al*., 1997, 2009; *Curran et al*., 2003; *Abram et al*., 2013]. Each of these records provides different perspectives on the variability of Antarctic sea-ice and the underlying processes involved. The longest available observational record is a fast-ice series from the South Orkney Islands, which we term the South Orkney Fast-Ice series: SOFI [*Murphy et al*., 1995]. Fast-ice occurs where sea-ice is attached to the coast or to other fixed features (e.g., ice walls, ice fronts, or grounded icebergs) [*World Meterological Organisation*, 1970; *Fraser et al*., 2012]. Analyses of fast-ice variability can provide insight into climate driven changes, but it is also an important part of Southern Ocean systems in its own right [*Murphy et al*., 1995; *Fraser et al*., 2012] as it influences the formation of Antarctic Bottom Water, the stabilization of glacier tongues and ice shelves and the operation of ecosystems [e.g., *Murphy et al*., 1995, 2007b; *Massom et al*., 2009, 2010; *Fretwell et al*., 2014]. Records of fast-ice provide potential insight into the relationships between local and regional sea-ice processes, extending analyses of natural variability and improving understanding of the regional impacts of Southern Hemisphere scale atmospheric variability associated with ENSO and SAM.

A previous analysis of fast-ice around the South Orkney Islands for the period from 1903 to 1994 showed that the duration of winter ice exhibited marked interannual and decadal variability, which was related to changes in SIE in the Weddell Sea and correlated with climate variability [*Murphy et al*., 1995]. Winter fast-ice duration is a function of the timing of both the formation and the breakout of ice, which have been shown to exhibit differing patterns of variability during the satellite era [*Stammerjohn et al*., 2008b; *Simpkins et al*., 2012]. The present study aims to extend and characterize the long-term record of fast-ice formation and breakout in the South Orkney Islands and investigate its association with large-scale Weddell Sea and wider Southern Ocean ice, ocean, and atmospheric variability. We derive a data set of formation and breakout times over more than a century based on two sets of historical observations [*Murphy et al*., 1995] and more recent camera images. We show that the timing of formation and breakout of fast-ice at the South Orkney Islands is representative of sea-ice conditions and processes in the wider Weddell and Scotia Sea region. We use spatial correlation and multivariate analyses to examine the local and regional climate and oceanic influences on the processes of formation and breakout during the satellite era. Finally, we examine how changes in the pattern of fast-ice variability over the last century are related to variations in atmospheric processes linked to ENSO and SAM.

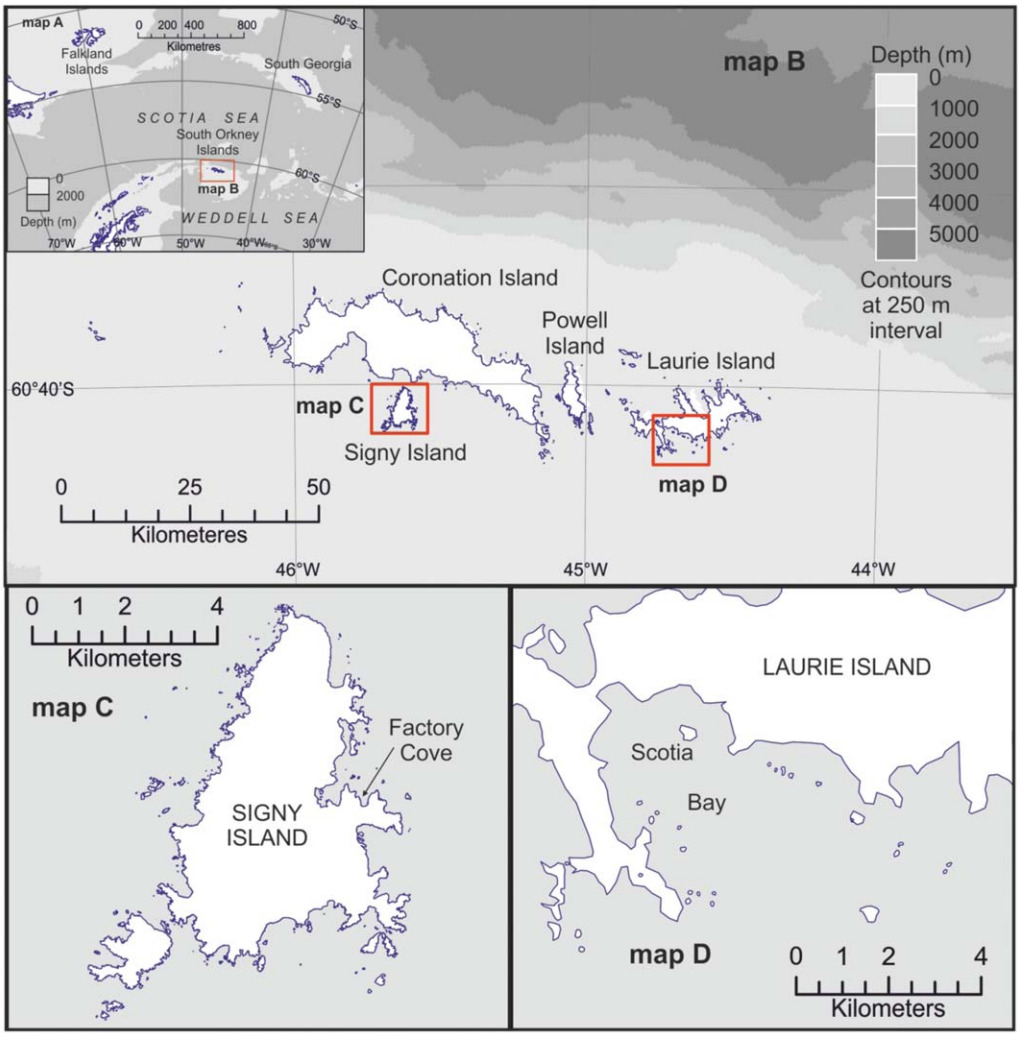

Figure 1. (a) Map showing the location of the South Orkney Islands in the Southern Ocean and (b) a detailed view of the South Orkney Islands showing the location of Signy Island and the Scotia Bay region of Laurie Island (red boxes). The two bottom panels show the locations of (c) Factory Cove on Signy Island and (d) Scotia Bay on Laurie Island where the fast-ice records were obtained.

2. Fast-Ice at the South Orkney Islands

The SOFI series is based on observations of the date of fast-ice formation and breakout from two bays on different islands in the South Orkney Islands group (approximately 60°40′S, 45°00′W) on the Southern Scotia arc at the northern edge of the Weddell Sea (Figure 1). The bays are Scotia Bay on Laurie Island and Factory Cove on Signy Island and are ~50 km apart (Figure 1). Signy Island is situated south of Coronation Island, the largest in the South Orkney Islands group, while Laurie Island lies to the east. Scotia Bay opens to the southeast and is formed by a low isthmus (<10 m elevation) that connects the main area of Laurie Island in the east to the peninsulas in the west. Factory Cove is more enclosed, opening to the north in the wider Borge Bay area. The local island topography is complex, and the large Moraine Valley area to the south is likely to be an important local influence on the regional winds acting at Scotia Bay.

These differences in geographic position and alignment may affect fast-ice responses to atmospheric and oceanic variability in the two bays. The SOFI series prior to 1947 is based on the Scotia Bay data and the Factory Cove data after that time. Between 1947 and 1975 data were recorded at both sites and *Murphy et al*. [1995] showed that the series were correlated during the overlap period (see below) and showed that the ice duration was approximately 23 days longer at Laurie Island than at Signy Island. They suggested that the offset between bays was likely the result of local topography and that their shared variability reflected the wider scale ice distribution and dynamics around the South Orkney Islands as a whole. However,

geographic influences may be a factor in any changes in fast-ice variability observed between the first and second half of the century.

The formation and breakout of fast-ice are affected by thermal and mechanical processes, but the exact mechanisms involved may be local and are often largely unknown. Cooling or warming associated with the atmosphere or ocean affect freezing and melt rates, while winds and waves generate break up of ice [*Crocker and Wadhams*, 1989; *Squire*, 1993; *Mahoney et al*., 2007a, 2007b; *Fraser et al*., 2012; *Petrich et al*., 2012]. The timings of formation and breakout of fast-ice in the South Orkneys are dependent on the seasonal development of the pack-ice, occurring, respectively, after arrival and retreat of the sea-ice [*Murphy et al*., 1995]. *Murphy et al*. [1995] suggested that fast-ice forms in Factory Cove when the temperature falls sufficiently low after the sea-surface has been stabilized by the arrival of the Weddell Sea pack-ice around the South Orkney Islands. They also suggested that the fast-ice breaks out rapidly after the first offshore (southerly) storm following the departure of the Weddell Sea pack-ice from the islands and when air temperatures had increased.

3. Data and Methods

3.1. The Updated Sea-Ice Data Series

Detailed descriptions of the SOFI data collection and analysis protocols used for the period prior to 1994 are given by *Murphy et al*. [1995]. Here we briefly note the main aspects and provide further detail for the post-1994 period. The first series ran from 1903 to 1975 and came from Scotia Bay (SB), Laurie Island. The second series came from observations from Factory Cove (FC) at Signy Island between 1947 and 1994. Both series were based on direct observations of the timing of the final complete autumn formation and spring breakout of ice from each of the bays (calculated as the number of days relative to the first of January each year). There was a significant correlation ($r^2 = 0.78$, $p < 0.001$) between the fast-ice duration series from SB and FC during the overlap period (1947–1975) [see *Murphy et al*., 1995, for further details]. In this analysis, we have recalculated the Scotia Bay and Factory Cove series and used dates of the final fast-ice formation and complete breakout as the primary data series and derived duration from those series. Occasional short periods of open water were ignored. This resulted in some changes to the SB duration series compared with the previous analysis and we note particularly the correction of the value for 1909 [cf. *Murphy et al*., 1995]. The 1928 and 1929 period was an extreme sea-ice year where there was no apparent summer breakout/reformation; values for these years were estimated using linear interpolation. During 1956 winter fast-ice did not form in FC; we therefore set both the formation and breakout dates for 1956 to day 226. This is the mean midpoint between all the formation and breakout dates, and since the dates of formation and breakout are identical, the calculated duration is zero, which is consistent with the observations. We note that 1956 was also an extreme low fast-ice year at SB, where duration was 42 days compared to a mean duration of 180 ($n = 67$, sd = 63, $CI_{0.05} = \pm 15.4$).

A range of methods were explored to compile a complete (1903–2008) series for the formation and breakout dates. These include calculating the mean difference (offset) between SB and FC data using all data from 1947 to 1975 inclusive, using just those years when data were available for both, and using geometric regression rather than mean offset to cross calibrate the data series. These different methodologies for linking the SB and FC data sets generate slight differences in the relative magnitudes of variability in the calibrated series and in the magnitude of change between the pre-1947 and post-1947 period. The mean offset method based on all available data between 1947 and 1975 maintains the same magnitude of change between pre-1947 and post-1947 (to 1975) period as in the original SB series [*Murphy et al*., 1995]. We applied a mean offset of −6 days to the fast-ice formation date at Scotia Bay, and of −28 days to the breakout date, in order to generate a complete SOFI series (Figure 2).

From the 1994/1995 austral summer, winter occupation of the research station ceased at Signy Island. To maintain the data series, the observation program was transferred to an automatic camera system using 35 mm film. The system was positioned at Observation Bluff (60°43′S, 45°36′W; 110 m) overlooking Factory Cove and generated a single image each day. During winter not all images were usable because of ice formation on the camera systems, but clear images were available for the formation and breakout periods. The images were examined to determine the date of ice formation, defined as the latest day when Factory Cove became completely frozen. It generally remained frozen throughout the winter, and occasional short periods of open water were ignored if the surface froze again completely. Previous analyses [*Murphy et al*., 1995],

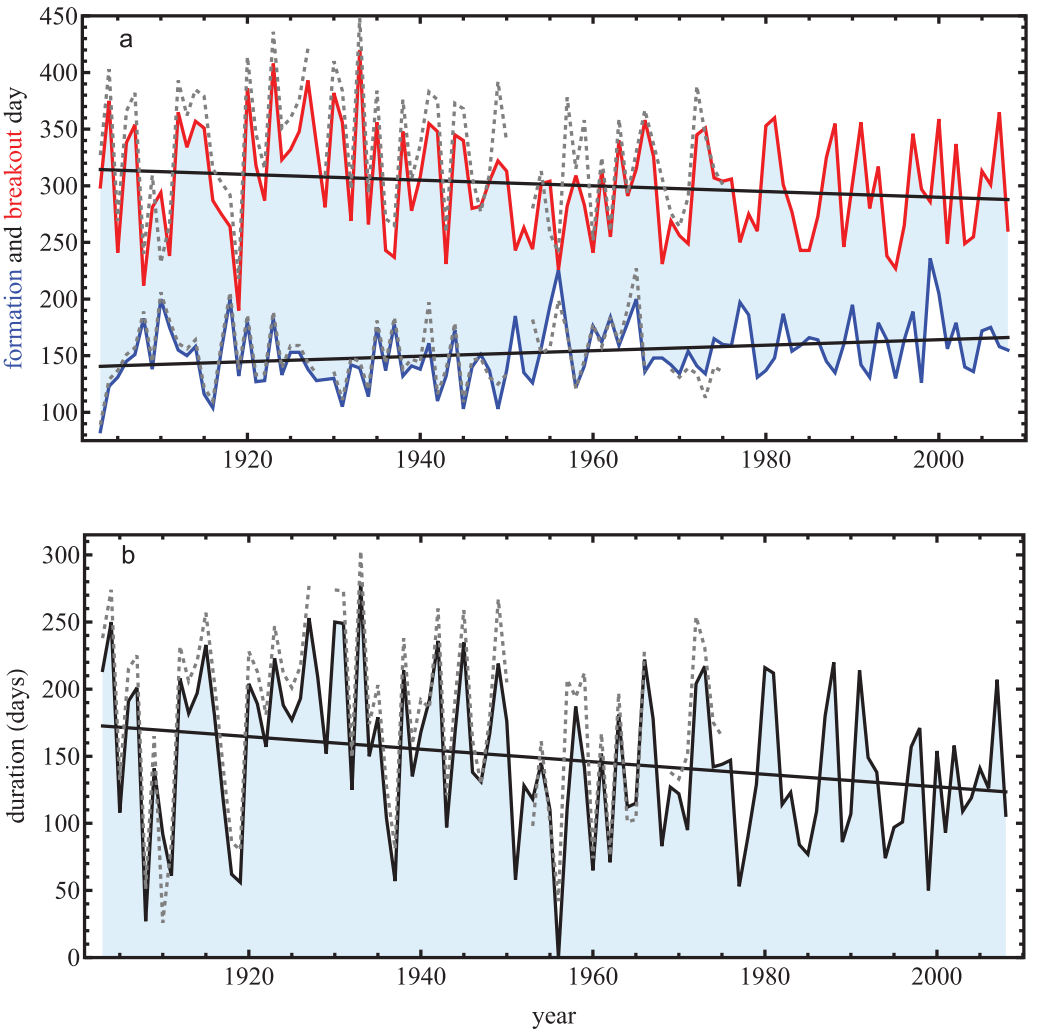

Figure 2. The combined SOFI fast-ice series for (a) formation (blue) and (b) breakout date (red) (relative to 1st January), and duration from the South Orkney Islands. Gray dashed lines show the respective Scotia Bay series. Trends for the SOFI series are shown, which are significant for the duration and formation series but not for breakout (Table 3).

indicated that comparison of fast-ice duration data including or excluding short periods of winter open water revealed no significant differences. The date of ice breakout was defined as the day when the ice finally cleared completely, and the bay remained clear of fast-ice for the summer. A system failure occurred in 2002 and no observational data are available for that year. In 2003, the system was replaced with a digital camera, which recorded two images per day (except for 2003–2004 when it recorded one image per day). Camera failures in 2009 and 2011 led us to limit the analyses to period from 1903 to 2008 for this study.

To derive estimates of fast-ice formation and breakout in 2002 (missing data), we compared the observed fast-ice data for the South Orkney Islands with the variability of sea-ice over a wider regional area. Here we used satellite SIC data [*Cavalieri and Parkinson*, 2008] for the period from 1979 to 2007 to derive time series for the date of arrival and departure of 15% SIC at Signy Island following the procedures given in *Stammerjohn et al.* [2008b]. For the 1979–2007 period, fast-ice formation ($n = 28$; mean day 160) occurs on average 57 days after the arrival of the 15% sea-ice edge around the South Orkney Islands, and fast-ice breakout ($n = 27$; mean day 292) 14 days after the sea-ice retreat. Regression relationships show significant correlations between the fast-ice formation and sea-ice arrival date ($74.74 + 0.83$ *arrival date*, $F = 47.73$, $n = 28$, $r = 0.80$, $p < 0.0001$) and fast-ice breakout and sea-ice retreat date ($101.37 + 0.69$ *retreat date*, $F = 16.36$, $n = 27$, $r = 0.63$, $p < 0.001$). These derived relationships were used to generate estimates of the fast-ice formation and retreat dates for FC in 2002. The complete formation, breakout, and duration SOFI series are shown in Figure 2, along with the Scotia Bay data for comparison.

Table 1. Fast-Ice Series: Mean Day of Formation and Breakout (Relative to 1st January) and Mean Durations[a]

Series	Formation Date (σ)	Breakout Date (σ)	Duration (days) (σ)
SOFI (1903–1946)	143 (26)	314 (55)	169 (62)
SOFI (1947–2008)	159 (26)	292 (40)	133 (49)
SOFI (1903–2008)	153 (27)	301 (48)	149 (57)

[a]Standard deviations are shown in parentheses.

Analyses of the relationships of the SOFI series with satellite ice and ocean and ERA-Interim atmospheric data were undertaken for the period from 1979 to 2008. For the SOFI data, we present analyses for the pre-1947 and post-1947 series (Table 1) when the Factory Cove series began, for the relationships between the SOFI series (Table 2) and the trends in the series (Table 3). Spatial correlation maps were derived based on relationships between the SOFI series and the variable values at each grid point.

4. Results

4.1. Correlations With Satellite Sea-Ice Records

Regional spatial coherence in the interannual variability of sea-ice in the Southern Ocean is well documented [e.g., *White and Peterson*, 1996; *Abram et al*., 2007; *Stammerjohn et al*., 2008b]. The duration of winter fast-ice in the South Orkney Islands has been shown to be closely associated with overall winter SIE across the Scotia Sea [*Murphy et al*., 1995]. To examine the extent to which the SOFI formation and breakout series reflect wider scale processes, we examined the spatial relationships with Southern Ocean SIC. The SOFI formation and breakout dates both show significant correlations with SIC in a broad area of the northern Weddell Sea and Scotia Sea regions, spanning an area 55–70°S and 50–15°W (blue-purple region in Figure 3a and Table 4). Significant correlations of fast-ice formation date with sea-ice in this region, with later fast-ice formation associated with lower ice concentrations (Table 4; $n = 30$; $p < 0.0001$), persist over the 10 month interval from November in the previous year to August, with the 3 month season of maximum correlations occurring from May to July. Fast-ice breakout date is significantly positively correlated with SIC (Table 4; $n = 30$; $p < 0.0001$) in the 55–70°S and 50–15°W region over a more restricted 3 month season spanning from September to November (Figure 3b, red region), with later breakout date associated with higher ice concentrations. The seasonal timings of maximum correlation coincide with the time of fast-ice formation (May–July) and breakout (September–November) at the South Orkney Islands. The correlations with satellite observations of SIC indicate that the SOFI series for ice formation and breakout are representative of regional-scale sea-ice behavior during the autumn advance and spring retreat of ice.

Fast-ice formation and breakout also show significant but inverse correlations ($n = 30$; $p < 0.05$) with sea-ice cover in the Amundsen Sea (Figure 3). This is an expression of the ADP and the opposing pattern in sea-ice conditions that exists between these two regions [*Abram et al*., 2007]. There is some indication that the correlations for fast-ice formation also extend in a narrow band along the western side of the Antarctic Peninsula (Figure 3a). This pattern of correlation may indicate that early winter ice formation processes around the northern tip of the Peninsula are influenced by processes operating in the northwestern Weddell Sea [see *Reiss et al*., 2009], as well as from the south and west of the Antarctic Peninsula [*Turner et al*., 2012].

4.2. Variability of South Orkney Fast-Ice

The SOFI formation date is less variable than the breakout date (standard deviations (sd) of 27 and 48 days, respectively) and contributes less to the year-to-year variation in duration (sd = 57 days) (Table 1). The mean day of formation occurs 16 days later ($p < 0.001$) in the post-1947 (when the FC series began) period ($n = 62$) compared to pre-1947 ($n = 44$), while the mean day of breakout occurs 22 days earlier ($p < 0.05$) and the mean duration is 36 days shorter ($p < 0.01$). It should be noted that the change in duration occurred during the period of overlap of the two series (1947–1975). The Scotia Bay series continued until 1975 and that shows a reduction of duration of 33 days between 1903–1946 and 1947–1975 periods ($p < 0.05$). There has been a significant decreasing trend ($p < 0.01$) in fast-ice duration over the whole series, which is due to both an increasingly earlier (not significant) breakout date and a significant trend ($p < 0.01$) toward later formation dates over the length of the South Orkney record (Table 3 and Figure 2). Overall this resulted in a reduction of the duration of winter fast-ice of approximately 5 days per decade over the last century. The lack of a statistically significant trend in the breakout date is notable, and highlights that the interannual variability of the breakout date is high and greater than that of the formation date (Tables 1 and 3). When

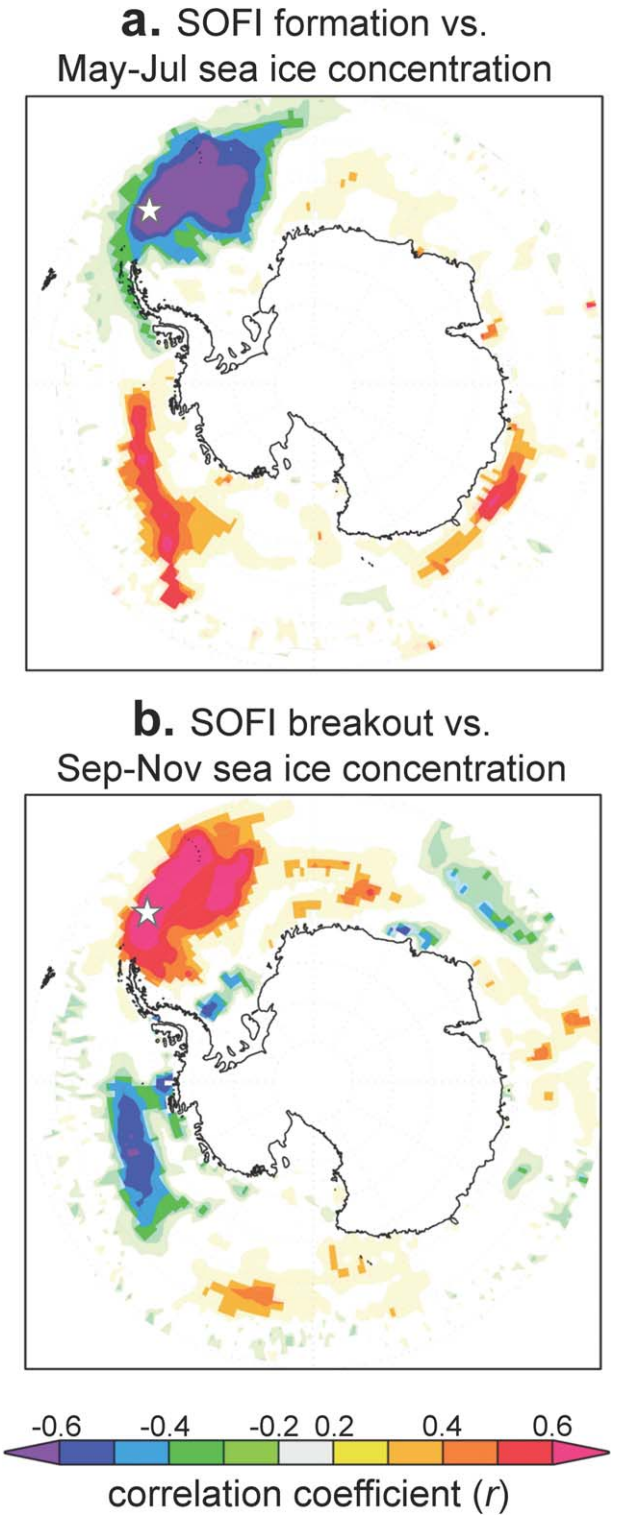

Figure 3. Spatial correlation of SOFI series with gridded satellite data for Antarctic SIC since 1979 [*Cavalieri and Parkinson*, 2008]. (a) SOFI formation date correlations with May–July averaged SIC, (b) SOFI breakout date correlations with September–November averaged SIC. Correlations with a statistical confidence less than 90% are masked, corresponding to absolute correlation coefficients exceeding 0.306 (95% level $r = 0.361$). Star denotes the location of the South Orkney Islands.

calculated only over the satellite era (1979 onward), the trends in fast-ice duration, arrival and departure are not significant (Table 3). This is consistent with satellite data that show no significant sea-ice trend in this region of Antarctica.

The winter duration of fast-ice at the South Orkney Islands over the 20th century was significantly correlated with both the date of fast-ice formation ($p < 0.0001$) and breakout ($p < 0.0001$), although the fast-ice breakout date is the stronger influence (breakout $r^2 = 0.79$ cf. formation $r^2 = 0.32$) (Table 2). Fast-ice breakout date is independent of the date of fast-ice formation earlier that same year (Table 2). There is, however, a statistically significant ($p < 0.01$), inverse relationship between fast-ice breakout date and the formation of sea-ice in the following year. This feature is not evident when the relationship is examined only over the satellite observation era since 1979.

With the high level of variability and autocorrelation in the fast-ice series it is important to understand how the patterns and periodicity of the sea-ice changes. We used wavelet analysis [*Torrence and Compo*, 1998] to investigate the periodicity and temporal persistence of fast-ice variability in the SOFI series. The duration series showed significant ($p < 0.05$; Figure 4) spectral power at periods of ~3–5, ~7–10, and ~15–20 years, although none are particularly persistent features (Figure 4) [see also *Murphy et al.*, 1995; *Abram et al.*, 2007]. Variability with ~15–20 years periodicity was significant during much of the first half of the South Orkney SOFI series, but has not been evident since ~1965 (Figure 4). The ~7–8 years periodicity that was present for over ~30 years between about 1965 and 1995 almost disappeared after the mid-1990s (Figures 2 and 4). This variability in duration reflects the dominance of ~7–8 years fluctuations in the breakout date during that time, a signal that was absent from the formation series (Figure 4). Higher frequency variability is a feature of both the formation and breakout series (Figures 4a and 4b). Fast-ice formation date shows variability primarily in the ~3–5 years band, and although not significant for the whole of the length of

Table 2. Correlation of Fast-Ice Series

Relationship	*n*	*r*	*p*
Full Series			
Duration versus formation	106	−0.57	<0.0001
Duration versus breakout	106	0.89	<0.0001
1979 Onward			
Duration versus formation	30	−0.38	0.12[a]
Duration versus breakout	30	0.85	<0.0001
Full Series			
Breakout versus formation (same year)	106	−0.12	0.705[a]
Breakout (*year 1*) versus formation (*year 0*)	105	−0.31	<0.01

[a]Not significant

the record, this does seem to be a relatively consistent feature of the fast-ice formation date. Variability was also significant at ~3–5 years during the first ~40 years of the breakout series.

As the major change in the SOFI series is detected during the period of data overlap between the Scotia Bay and Factory Cove series (1947–1975), we have also examined the consistency of the signals in the Scotia Bay series alone. The record is short, but wavelet analyses of the Scotia Bay series (not shown) show a very similar pattern to that observed in the full SOFI series, and the same frequencies dominate during the period of overlap (Figures 2 and 4). To examine whether the major step-change signal has been maintained in the full SOFI series, we applied a sequential analysis algorithm developed to detect regime changes in time series data [*Rodionov*, 2004, 2006]. Focusing on the long-term changes, we applied a cutoff length of $l = 25$, a Huber parameter of 1 and a probability level of $p = 0.05$. The analyses were not sensitive to changes in the Huber parameter, the cutoff length *l* for values greater than 15, or the method of prewhitening. Here we report the analyses using the Inverse Proportionality with four corrections method (IP4) described in *Rodionov* [2006].

The regime shift analyses identified a significant change ($p < 0.05$) in the SB mean breakout date and duration centred on 1951 (cutoff length $l = 25$). The analyses also suggested that were also significant changes ($p < 0.05$) in the last few years of the series (after 1969), which reflected shorter-term variation rather than a change in the long-term mean. Analyses of the full SOFI series also shows that the change in the breakout date and duration occurred around 1951. The full SOFI series also identified a change on the timing of formation in the 1950s (1954). Although the analyses identify a specific year, we note that the window applied is wide (25 years) and that moving average analysis indicates the change occurred over a period from about 1945 to 1965 [*Murphy et al.*, 1995]. The analyses indicate that SB and SOFI series both show the same major change in fast-ice during the mid-20th century, and suggest that the process of creating the full SOFI series has produced a series with the same major properties observed in the SB series during the period of data overlap.

4.3. Relationship to Meteorological and Oceanographic Conditions

To consider the role that oceanic and atmospheric processes play in the variability of sea-ice in this region, we examined the relationships between the SOFI series and spatial fields of SST [1982–2008, *Reynolds et al.*, 2002] and atmospheric parameters [1979–2008, ERA-Interim, *Dee et al.*, 2011]. Correlation patterns of fast-ice with SST and air temperatures (Figure 5) are similar to those for the SICs (Figure 3). For fast-ice formation, correlations with regional ocean temperatures (SST) in the northern Weddell Sea (55–70°S, 50–15°W) are again strongest in May–July ($p < 0.0001$), with later formation associated with warmer ocean temperatures (Figure 5b and Table 4). In September–November, later fast-ice breakout is associated with cooler ocean temperatures ($p < 0.0001$) (Figure 5d and Table 4). These periods of maximum correlation coincide with the seasonal timings of formation and breakout, respectively, and for SST are stronger for formation than breakout ($r = 0.82$ cf. $r = -0.66$; Table 4).

Table 3. Trends in Fast-Ice Series

Series	n	p	Trend (±se) (Days per Decade)
1903–2008			
Formation	106	<0.01	2.4 (0.8)
Breakout	106	<0.097[a]	−2.5 (1.5)
Duration	106	<0.01	−4.7 (1.8)
1979–2008			
Formation	30	0.286[a]	5.8 (5.3)
Breakout	30	0.963[a]	−0.4 (9.4)
Duration	30	0.540[a]	−6.2 (10)

[a]Not significant.

For fast-ice formation, the correlation patterns with SST are long-lived features that are significant ($p < 0.0001$) from October in the previous year through to August (Table 4). The same positive relationship is shown with air temperatures and persists over the January–June period (all months significant, $p < 0.05$), and is most significant for the 3 month May–July period ($r = 0.54$, $p < 0.01$; Table 5). The date of fast-ice formation shows little

Table 4. Correlation of Fast-Ice With Oceanographic and Sea-Ice Variables

Relationship		n	r	p
Sea-Ice Concentration (SIC) in Region 55–70°S, 50–15°W				
Maximum 3 months				
Formation versus regional sea-ice	May to Jul	30	−0.77	<0.0001
Breakout versus regional sea-ice	Sep to Nov	30	0.80	<0.0001
Whole significance period				
Formation versus regional sea-ice	Nov to Aug	30	−0.76	<0.0001
SST in Region 55–70°S and 50–15°W				
Maximum 3 months				
Formation versus regional SST	May to Jul	27	0.82	<0.0001
Breakout versus regional SST	Sep to Nov	27	−0.66	<0.001
Whole significance period				
Formation versus regional SST	Oct to Aug	26	0.81	<0.0001
Breakout versus regional SST	Sep to Dec	27	−0.67	<0.0001

relationship with zonal winds (Figure 6b) or meridional winds (Table 5), but occurs later when high atmospheric pressures dominate in the South Atlantic (Figure 6a). These results suggest a preconditioning effect over the previous year, and that formation date is affected by conditions during the preceding summer [see also, *Turner et al*., 2012], with winds and pressure systems playing a secondary role nearer to the fast-ice formation date.

For fast-ice breakout, the significant correlation patterns with SST exist from September to December ($p < 0.001$; Table 4) and the areas of correlation are restricted to a narrow band along the southern Scotia arc (Figure 5d), which is the main area of the spring marginal ice zone in the Scotia Sea [*Murphy et al*., 2007a]. This indicates that SST in this area is mainly dependent on the presence or absence of sea-ice, and hence on the timing of ice retreat, rather than thermal processes in the ocean, which would have a signature across the whole region as seen in the air temperatures and in the May–July SST (cf. Figures 5a and 5c and 5b and 5d).

Fast-ice breakout date is associated with the near-surface meteorological conditions during September–November (Figures 5c and 6c), with later fast-ice breakout associated with colder air temperature anomalies across the Weddell Sea (Table 5; maximum 2 months September–October, $r = -0.71$, $p < 0.0001$). There are also significant negative/positive relationships with the zonal/meridional winds, which are again strongest during September–October (Table 5), with maximum values in September and the correlation strongest with zonal winds ($n = 30$; zonal $r = -0.69$, $p < 0.0001$; meridional $r = -0.44$, $p < 0.05$). This indicates that breakout is earlier when there are stronger westerly/north-westerly winds during September. This is consistent with the spatial correlation analysis of breakout date with MSLP and zonal winds, which show that later fast-ice breakout dates are associated with high mean sea level pressure anomalies to the west of the Antarctic Peninsula in the ABS region, and low sea level pressure anomalies in the Southern Ocean surrounding the Antarctic continent (Figure 6c). Delayed fast-ice breakout also occurs in years when westerly wind anomalies in a band surrounding the Antarctic continent are reduced (i.e., the westerly winds are weaker) (Figure 6d). Together the atmospheric spatial correlations show patterns around the Antarctic region that resemble the SAM. They suggest that later fast-ice breakout may be associated with a reduced SAM index in spring.

To examine the regional atmospheric influences on fast-ice in more detail, we derived composite MSLP anomaly maps for the day of fast-ice formation each year for the period from 1979 to 2008 (relative to the May–August MSLP; Figure 7a). The MSLP anomaly map shows that at the time of formation strong, cold southerly winds occur across the western Weddell Sea. This arises due to high pressure anomalies over the ABS region and low pressure anomalies over the eastern Weddell Sea. The South Orkney Islands lie between these pressure centers and the associated southerly winds would bring cold air into the bays where sea-ice forms. For breakout, we used the September MSLP field as the climatology. The MSLP anomaly map for fast-ice breakout (Figure 7b) shows a deep low pressure anomaly west of West Antarctica. This produces a strong westerly to north-westerly flow through the Drake Passage, bringing warmer air from lower latitudes onto the tip of the Antarctic Peninsula and the northern Weddell Sea region around the South Orkney Islands.

4.4. Lag Correlations

Oceanic and cryospheric anomalies that propagate eastward in association with the Antarctic Circumpolar Current (ACC) are known to influence Scotia Sea variability [*Murphy et al*., 1995; *White and Peterson*, 1996;

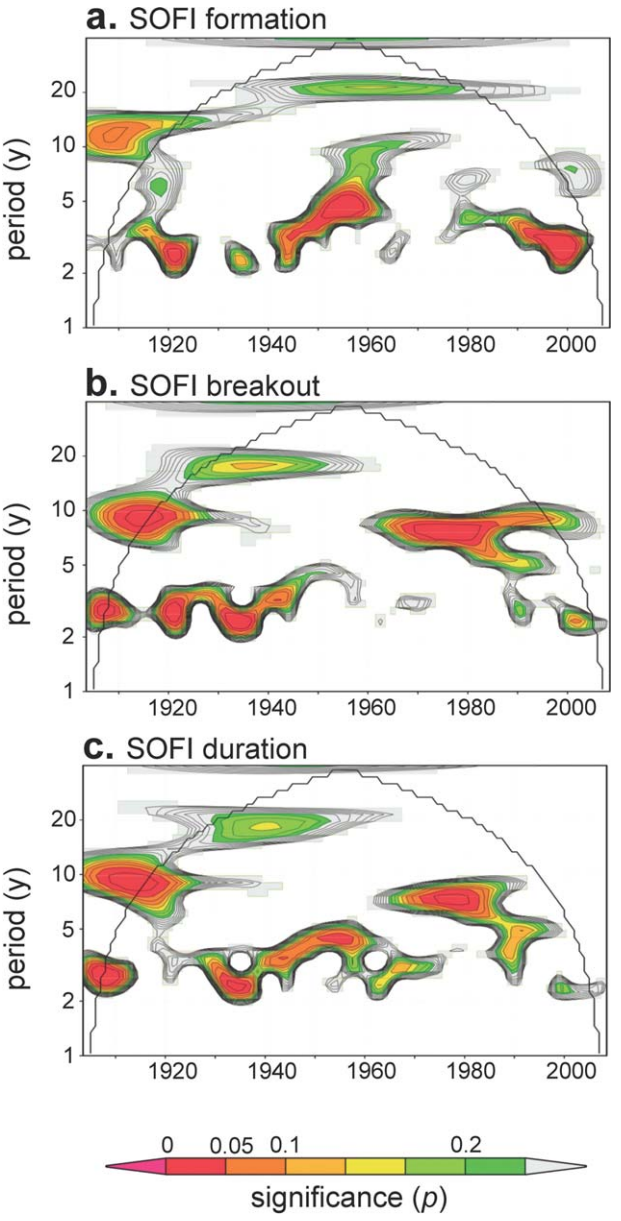

Figure 4. Wavelet power spectrum for the SOFI series showing the time evolution of variance of (a) formation date, (b) breakout date, and (c) duration [*Torrence and Compo*, 1998]. The analysis used a Morlet 6 transform and wavelet power is shaded based on statistical significance. Curved windows show the cone of influence, outside of which wavelet power may be influenced by padding of the time series.

Holland and Raphael, 2006; *Meredith et al*., 2008; *Yuan and Li*, 2008]. To examine the influence of propagating sea-ice anomalies on fast-ice variability in the Northern Weddell Sea, we derived lagged correlation maps. Lagged correlations of SIC with the SOFI formation date show a dipole between the Amundsen-Bellingshausen and Weddell Sea regions 18 months before the fast-ice formation (Figure 8). The correlation patterns with sea-ice 18 months previously are of opposing sign to those seen at the time of fast-ice formation. The correlation with the sea-ice anomaly in the Amundsen Sea is then seen to progress eastward across the Bellingshausen Sea and around the Antarctic Peninsula into the northern Weddell Sea. This is consistent with the anomaly propagation observed in SST shown by *Meredith et al*. [2008]. However, the sea-ice analysis also shows a propagation signal within the Weddell Sea. At 18 months lag (Figure 8d), negative correlations with SIC are seen in the southern Weddell Sea, which then migrate northward to the region of maximum sea-ice correlations around South Orkney. Combined with the earlier evidence that sea-ice arrival is being influenced by preconditioning from preceding sea-ice and SST conditions (rather than just atmospheric forces), this suggests that the 3–4 years periodicity in the fast-ice formation date is most likely derived from the propagation of anomalies from the Amundsen/Bellingshausen Seas and around the Weddell Gyre. This represents the time that it takes for sea-ice anomalies of the opposite sign (associated with the Antarctic Dipole), to migrate from the Bellingshausen Sea to the northern Weddell Sea, as well as from the southern Weddell Sea.

This migrating influence of opposite signed anomalies associated with the variation between the Amundsen/Bellingshausen Sea and Weddell Sea regions does not appear to be a significant contributor to variability in the fast-ice breakout date over the satellite observation era (Figure 9). Sea-ice correlations of an opposite sign are observed over the South Orkney region of the Weddell Sea four years (i.e., half of the ~7–8 years periodicity) before the maximum September–November correlation with fast-ice breakout. But unlike the migrating correlations observed for fast-ice formation, no correlation features are observed in lagged correlations over 3 to 1 year lags. This suggests that the variability in fast-ice breakout in the ~7–8 years period is a

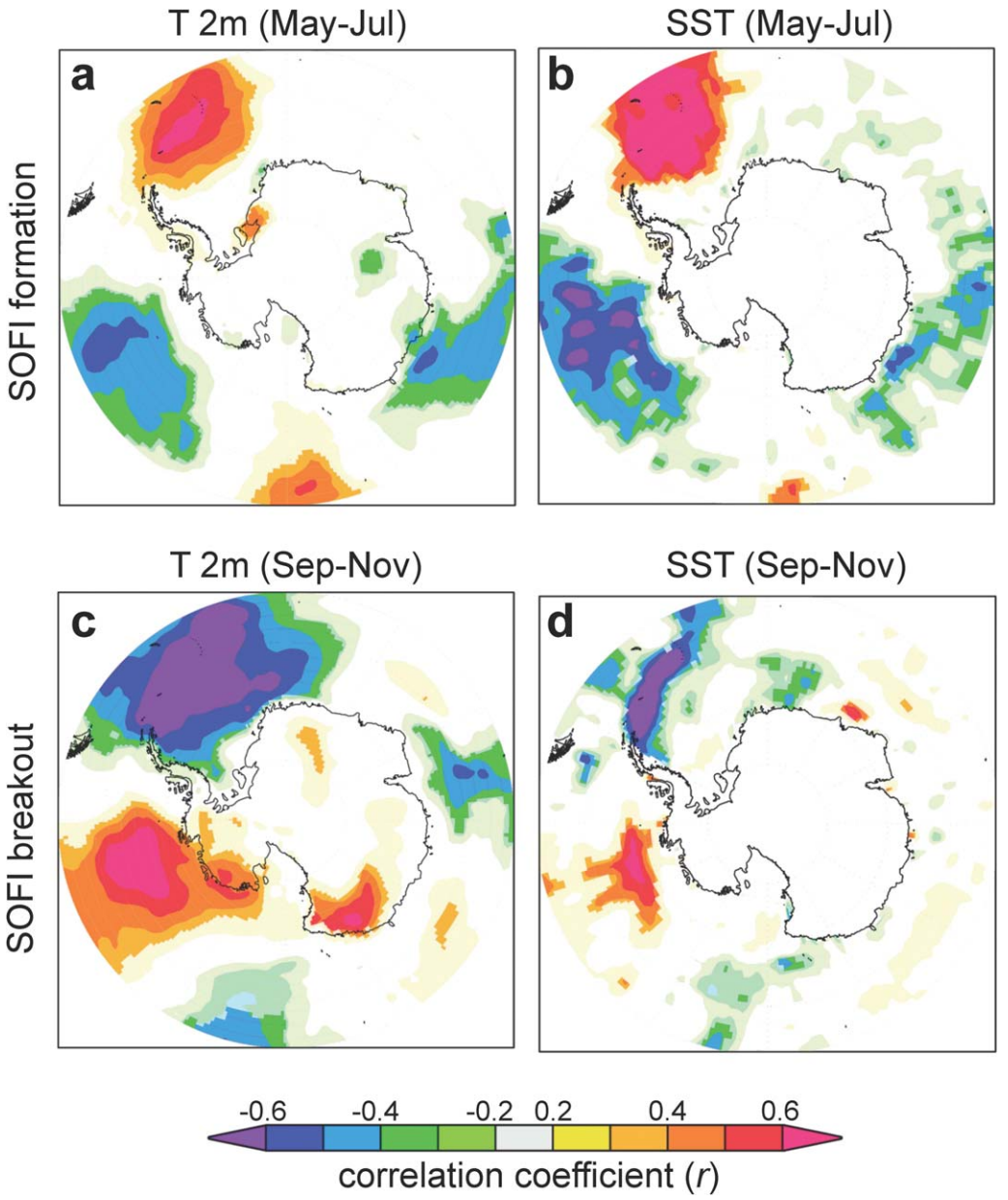

Figure 5. Spatial correlation of SOFI series with gridded ERA-Interim 2 m air temperature (T2m) data since 1979 [*Dee et al.*, 2011] and sea surface temperature (SST) data since 1981 [*Reynolds et al.*, 2002]. SOFI formation date correlations with May–July averaged (a) T2m and (b) SST. SOFI breakout date correlations with September–November averaged (c) T2m and (d) SST. Correlations with a statistical confidence less than 90% are masked.

feature imparted mainly through external climate variability that influences the spring breakout of fast-ice at South Orkney, rather than an internal feature of sea-ice/ocean processes in this region.

4.5. Relationships With ENSO and SAM

To examine the influence of ENSO and SAM variability on sea-ice, we use the SAM index (1957–2008) developed by *Marshall* [2003] and the NINO3.4 SST index (1903–2008) [*Kaplan et al.*, 1998]. Fast-ice formation and breakout both have significant correlations with ENSO variability. These correlations begin in April of the previous year and persist into the start of the year of fast-ice formation and breakout at the South Orkneys (Figure 10). Lag analysis shows that both fast-ice formation and breakout date show the strongest correlations with NINO3.4 SST in June–August of the previous year (Figure 10 and Table 5), although it is much stronger for the formation date ($n = 105$; $r = -0.46$; $p < 0.0001$) than the breakout date ($n = 105$; $r = 0.26$;

Table 5. Correlation of Fast-Ice With Atmospheric Variables

Relationship		*n*	*r*	*p*
ERA-Interim in Region 55–70°S, 50–15°W				
	Months			
Formation				
Formation versus air temperature 2 m	May to Jul	30	0.54	<0.01
Formation versus zonal winds	May to Jul	30	0.05	NS
Formation versus meridional winds	May to Jul	30	−0.08	NS
Breakout				
Breakout versus air temperature 2 m	Sep to Oct	30	−0.71	<0.0001
Breakout versus zonal winds	Sep to Oct	30	−0.56	<0.01
Breakout versus meridional winds	Sep to Oct	30	0.59	<0.001
Niño 3.4 in Previous Year				
	Maximum 3 months			
Formation versus Niño 3.4	Jun to Aug (lag 12)	105	−0.46	<0.0001
Breakout versus Niño 3.4	Jun to Aug (lag 12)	105	0.26	<0.01
SAM [Marshall, 2003]				
Breakout versus SAM	Sep	52	−0.38	<0.01

$p = <0.01$). Correlations with conditions several months earlier point to an interaction between sea-ice variability at South Orkney and tropical ENSO variability that is propagated through the oceans (rather than the atmosphere).

To understand the impacts of ENSO in more detail requires consideration of different phases of the ENSO cycle [*Meredith et al*., 2008; *Stammerjohn et al*., 2008b]. Composite SST anomaly plots where constructed for El Niño (1982, 1987, 1991, 1997, 2002, 2004) and La Niña years (1985, 1988, 1998, 1999) based on classification by the NOAA Climate Prediction Centre (Figure 11). Plots were constructed for June–August of the El Niño and La Niña years (where maximum lagged correlations exist with South Orkney fast-ice), as well as the following September–November, May–July + 1, and September–November + 1 (+1 = following year). These months were chosen to correspond to the timing of fast-ice breakout and formation at South Orkney. The SST anomalies that formed in the Pacific sector of the Southern Ocean during El Niño and La Niña events persist through the following year and migrate from the Bellingshausen Sea through Drake Passage and into the northern Weddell Sea. Regional SST and sea-ice conditions are closely correlated [*Murphy et al*., 1995; *White and Peterson*, 1996; *Meredith et al*., 2008] and this ocean propagation likely accounts for the correlation of SOFI anomalies with ENSO in the previous year (Figure 11).

Correlations with the SAM index [*Marshall*, 2003] are significant for fast-ice breakout, but only for the month of September (Figure 10 and Table 5) which coincides with the start of the sea-ice retreat in this region. This short interval of correlation suggests a transient connection between SAM and fast-ice breakout, whereby it is the strength of the SAM circumpolar westerly winds at the time of ice breakout that influence the variability in breakout date. This view is supported by the spatial correlation of fast-ice breakout to SAM-like pressure and zonal wind patterns that only persists during the time of ice breakout (Figures 6c and 7b). There is no correlation of fast-ice formation with SAM.

Using the extended sea-ice series provided by the SOFI data, we also examine the temporal consistency of the relationship with ENSO and SAM. To examine the long-term correlations with SAM over the 20th century we use the *Fogt et al*. [2009] series in addition to the *Marshall* [2003] series using mean values for September–November. We note that using the combined series in this way involves data from the two different localities (Scotia Bay and Factory Cove). It is possible that local effects considered above may mean that atmospheric changes associated with ENSO and SAM variability may differ between the two regions. Using 25 year moving correlation windows, we find that the fast-ice formation relationship with ENSO (in the previous year) weakened between ~1925–1945 and ~1965–1985 to below the 95% confidence interval (Figure 12a). The earlier period corresponds with a well-documented interval when ENSO variability and teleconnections were subdued [*Cole et al*., 1993; *Urban et al*., 2000], supporting suggestions that the influence of ENSO on sea-ice in the South Orkney region is strongest when ENSO itself is strong [*Stammerjohn et al*., 2008b].

For fast-ice breakout, the association with ENSO is generally weaker and the moving 25 year correlation analysis indicates that this association was only significant above the 95% confidence interval between

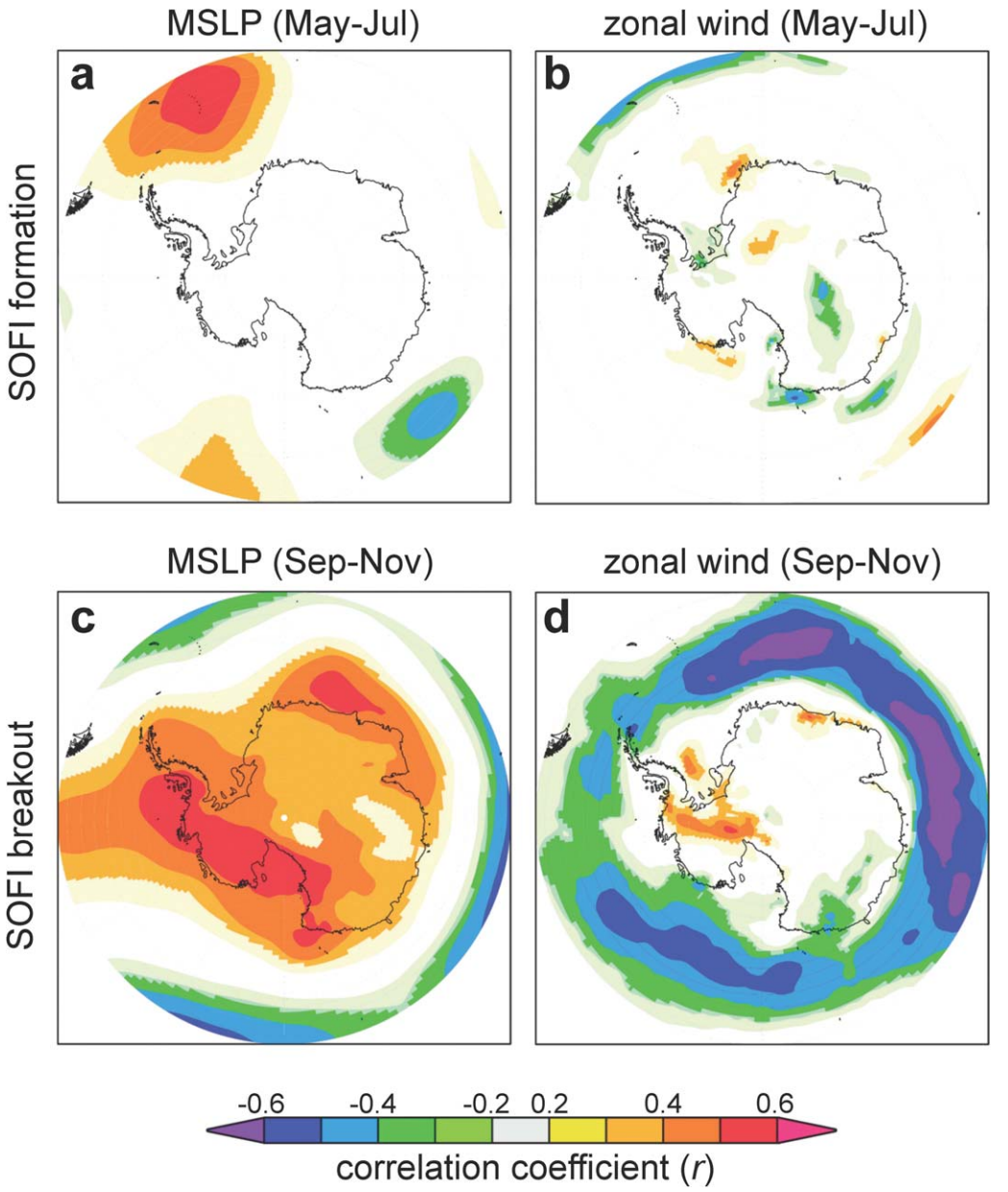

Figure 6. Spatial correlation of SOFI series with gridded ERA-Interim mean sea level pressure (MSLP) and zonal wind fields since 1979. SOFI formation date correlations with May–July averages of (a) MSLP and (b) zonal winds, and SOFI breakout date correlations with September–November averages of (c) MSLP and (d) zonal winds. Correlations with a statistical confidence less than 90% are masked.

~1935 and 1955 (Figure 12b). Breakout date has shown an increased negative correlation with the SAM (later breakout associated with negative SAM) since 1957 when the *Marshall* [2003] SAM series started. The correlation with the extended SAM series indicates that a negative (but not significant) relationship with breakout existed throughout much of the 20th century (Figure 12c), and further highlights the recent strengthening impact of SAM on fast-ice breakout.

4.6. Influences on the Timing of Formation and Breakout of Fast-Ice

To further examine the major covariates associated with formation and breakout of fast-ice from the South Orkney Islands, we undertook a series of multivariate analyses. For the period from 1982 to 2007, we derived a series of annual and monthly variables and 1 year lag series for ENSO, SAM, SST, and SIC. Preliminary correlation analyses were used to identify highly correlated variables to avoid issues of

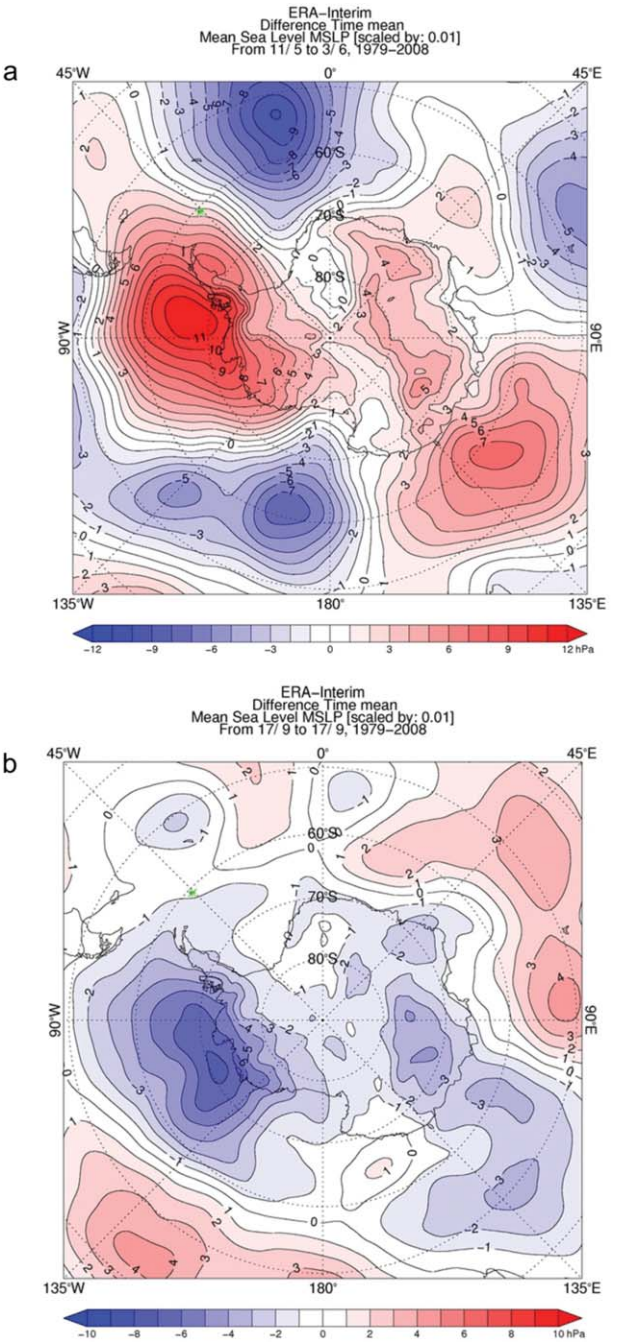

Figure 7. Mean anomaly plot of mean sea level pressure (MSLP) over the period from 1979 to 2008 on the day of (a) formation and (b) breakout. The Green dot marks the location of the South Orkney Islands.

multicollinearity. There was no evidence of non-Gaussian error distributions of the covariates. We generated Generalised Linear Models with linear and quadratic responses with Gaussian errors and selected the lowest Akaike Information Criteria (AIC) values to identify the best (most parsimonious) model and the main covariates [*Burnham and Anderson*, 2002].

For the formation date, the best model was a quadratic function of SST during May with an additional ENSO-related term:

$$formation\ \ day = 524.56 + 81.474\, SST_{may}{}^{***} + 32.633\left(SST_{may}\right)^{2\ NS} - 12.049\, ENSO_{-1}{}^{**}$$

The model explained 76.2% (adjusted r^2; $p < 0.0001$; ** significant at 5% level; *** 1% level; NS = not significant) of the variation in the formation series. The major covariate is the SST during May, which alone explains 63.9% of the variation ($p < 0.0001$). The inclusion of the SST^2 term indicates a weak (but not significant) nonlinear response to SST. The regional SST and SIC data are highly negatively correlated ($r^2 = 0.83$, $p < 0.0001$) indicating that the general seasonal development of the ocean and sea-ice conditions around the South Orkney islands during autumn is the major determinant of the timing of the formation of fast-ice in Factory Cove. However, the inclusion of the influence of variation in ENSO the year before the date of formation further supports the suggestion from the circumpolar analyses that wider scale and longer term conditions over the previous 12–18 months are also important in preconditioning the sea-ice system.

For the breakout date, the best model included just the SST and the SAM index during September:

$$breakout\ \ day = 201.313^{***} - 88.910\, SST_{sep}{}^{***} - 10.704\ SAM_{sep}{}^{**}$$

The model explained 54.6% (adjusted r^2; $p < 0.0001$) of the variation in the formation series, with the major covariate being the SST during September, which explained 36.1% of the variation ($p < 0.0001$). The model highlights the importance of the combined effects of the general regional SST and ice conditions and the wind stress during the spring. We note that the multivariate analysis is conducted over a time interval when breakout was not significantly correlated with ENSO (Figure 12b). However, at other times during the last century ENSO may have also been an important aspect of the multivariate influences on fast-ice breakout.

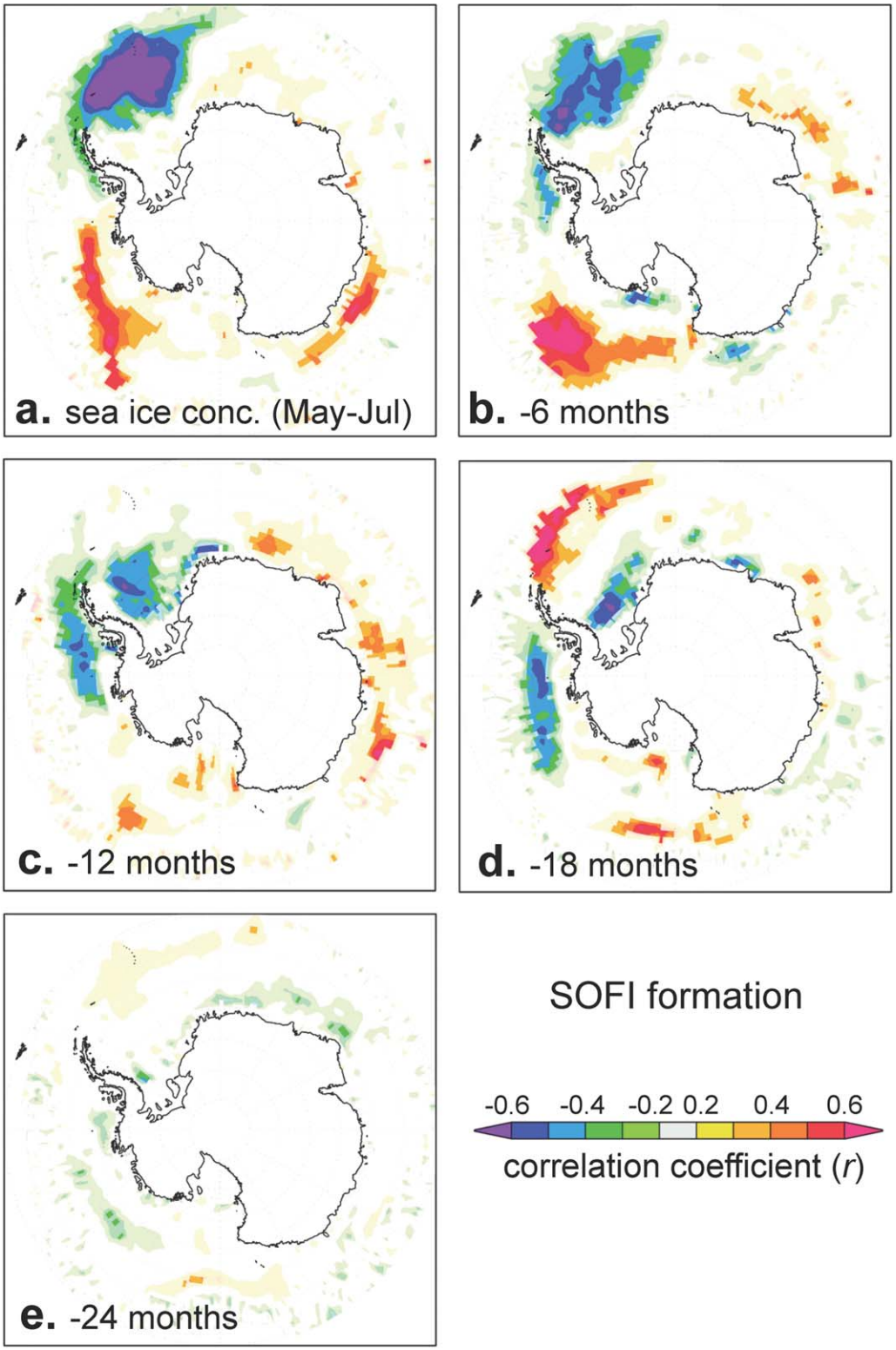

Figure 8. Lagged spatial correlations of SOFI formation date with gridded satellite data for Antarctic SIC since 1979 [*Cavalieri and Parkinson*, 2008]. SOFI formation date correlations with SIC are shown for (a) the maximum May–July interval (as in Figure 3a), and for SIC in the previous (b) 6 months, (c) 12 months, (d) 18 months, and (e) 24 months. Correlations with a statistical confidence less than 90% are masked.

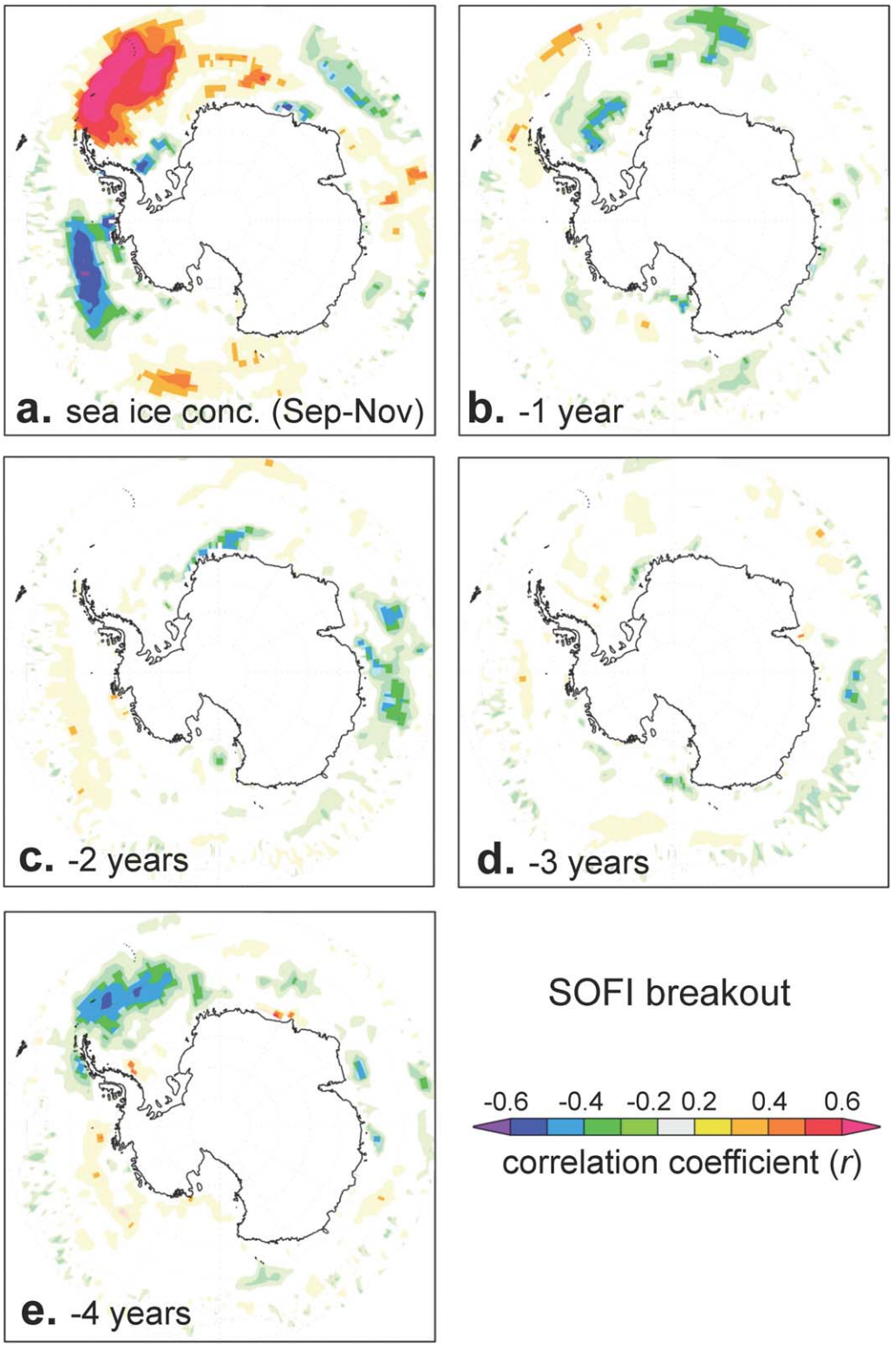

Figure 9. Lagged spatial correlations of SOFI breakout date with gridded satellite data for Antarctic SIC since 1979 [*Cavalieri and Parkinson*, 2008]. SOFI breakout date correlations with SIC are shown for (a) the maximum September–November interval (as in Figure 3b), and for SIC in the previous (b) 1 year, (c) 2 years, (d) 3 years, and (e) 4 years. Correlations with a statistical confidence less than 90% are masked.

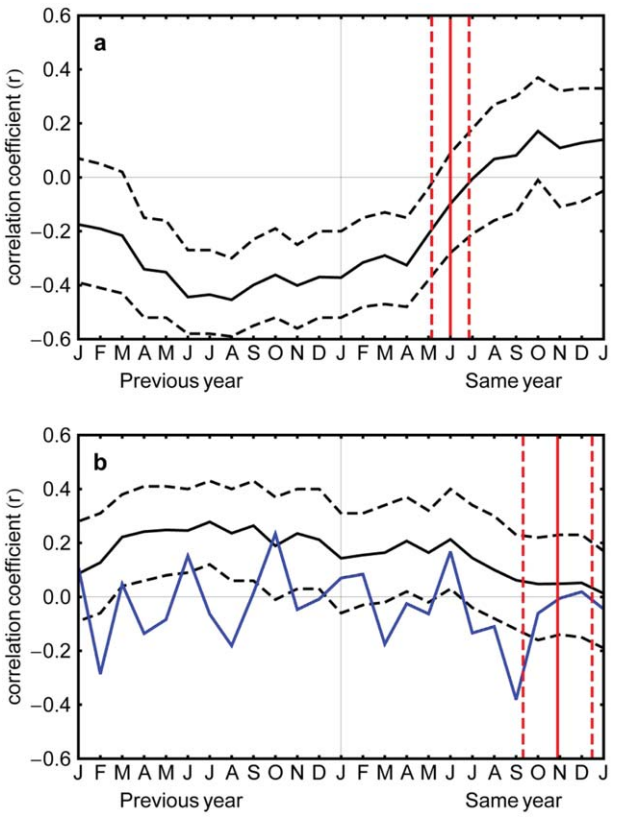

Figure 10. Correlation (*r*) of (a) fast-ice formation and (b) fast-ice breakout with NINO3.4 SST (black) [*Kaplan et al*., 1998] and SAM index (blue) [*Marshall*, 2003]. Solid black lines give monthly *r* values at lags from January in the previous year through to January after the year of fast-ice formation and breakout. Dashed black lines give 95% confidence interval for the lagged correlations, which are significant when the window does not include $r = 0$. Correlations with SAM are only significant for fast-ice breakout during September immediately preceding breakout. Solid (dashed) vertical red lines indicate the mean (standard deviation) timing of sea-ice formation and breakout.

5. Discussion

5.1. Variability of Breakout and Formation of Fast-Ice in the South Orkney Islands

The processes of formation and breakout of fast-ice in the South Orkney Islands are influenced by factors operating at local, regional, and Southern Hemisphere scales. Local fast-ice breakout and formation are preceded by regional spring retreat and warming, and autumn advance and cooling, respectively. Fast-ice breakout at the South Orkney Islands occurs after the retreat of the winter sea-ice from the region. Locally, when the sea-ice clears, the ocean swell can develop, which fractures and breaks up the fast-ice and causes it to become detached from the coast [*Squire*, 1993; *Crocker and Wadhams*, 1989; *Petrich et al*., 2012]. The regional analysis showed that breakout date at Factory Cove is correlated with the near instantaneous impact of the spring zonal winds and occurs earlier during periods when westerly winds are stronger.

In contrast to the association of ice breakout with instantaneous atmospheric conditions, the timing of fast-ice formation is also influenced by processes over longer time scales and across a much larger region. Warmer conditions in the central tropical Pacific are associated with an earlier advance of ice across the Scotia Sea during the autumn as a result of the stronger southerly meridional winds along the eastern Antarctic Peninsula, cooler conditions and stronger drift of sea-ice northward [*McKee et al*., 2011]. This is demonstrated by the intense high MSLP anomaly to the west of the Antarctic Peninsula, which brings cold air north from the continent at the time of fast-ice formation (Figure 7a). When the sea-ice edge is north of South Orkney Islands, the associated general cooling and reduced ocean swell will allow fast-ice to form. However, these meteorological conditions act in conjunction with persistent anomalies in ice concentration (and SST) over the previous 12–18 months that migrate from the Bellingshausen Sea region and around the Weddell Gyre. This builds on previous studies of Weddell Sea-ice variability, which have shown a quasi-quadrennial cycle of ice propagation around the Weddell Gyre associated with the ADP variability [*Venegas and Drinkwater*, 2001]. The persistence of a 3–5 years periodicity in the SOFI formation series suggests that the quasi-quadrennial cycle is a robust feature of the ice dynamics in this part of Antarctica.

The analyses show that the SOFI series is representative of the sea-ice variability in the wider Weddell and Scotia Sea region. Variation in breakout date is greater than the formation date and therefore dominates the variability of duration and regional changes in ice concentration [cf. *Stammerjohn et al*., 2008b]. Regional atmospheric, oceanic, and sea-ice variability influence the timing of advance and retreat across the Weddell Sea and that is crucial to determining the formation and breakout in the South Orkney Islands. The SOFI series thus provides a long-term observational record of regional sea-ice variability to better assess the influence of regional variation associated with ENSO and SAM climate modes on the interannual fluctuations in sea-ice.

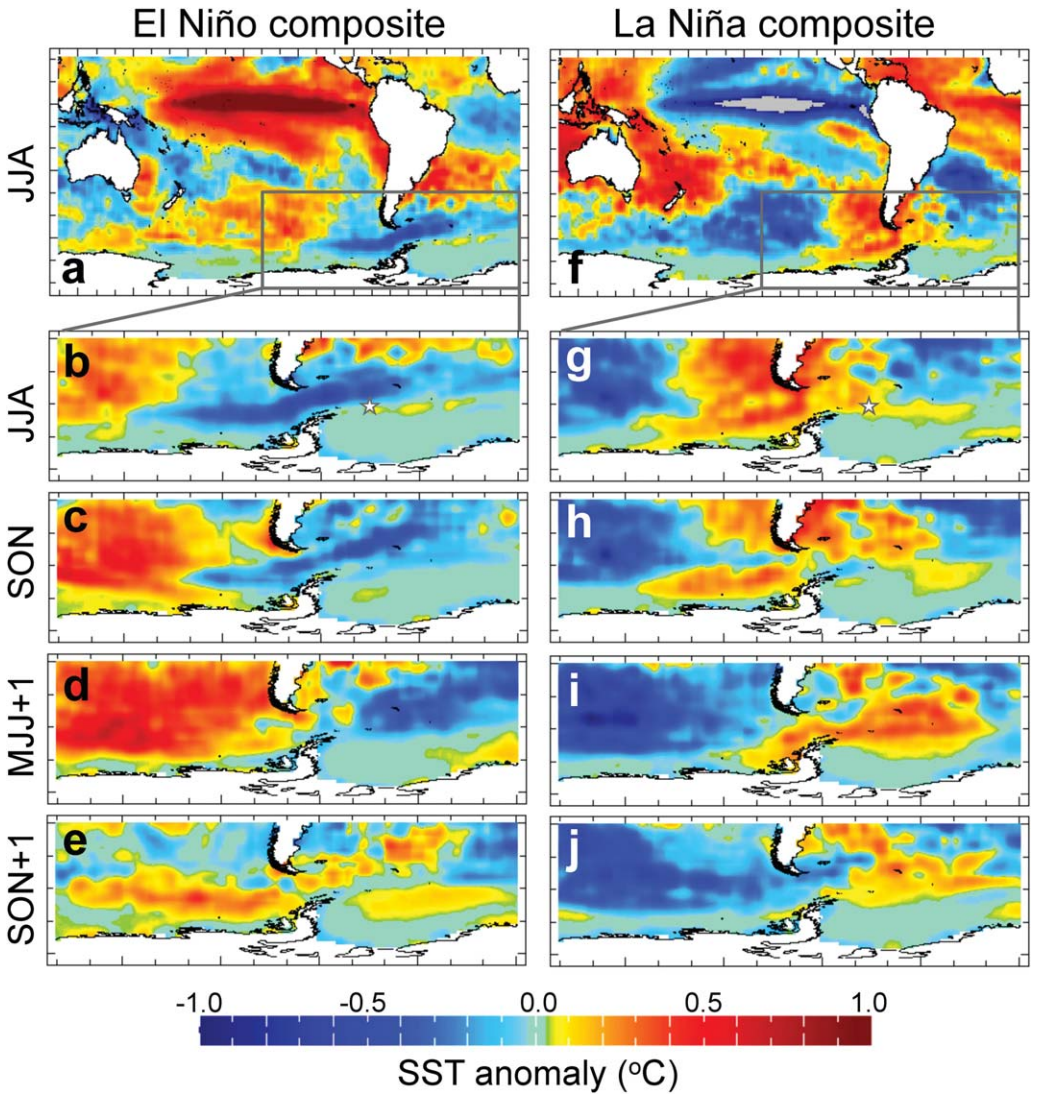

Figure 11. Composite SST anomaly [*Reynolds et al*., 2002] maps for El Niño and La Niña events since 1981. El Niño composites are shown for (a) June–August averages of the 1982, 1987, 1991, 1997, 2002, and 2004 events. (b–e) A closer view of El Niño SST anomalies propagating through the Drake Passage region, for (b) June–August, (c) September–November, (d) May–July of the following year, and (e) September–November of the following year. (f–j) Same as Figures 11a–11e, but for La Niña composites for the 1985, 1988, 1998, and 1999 events. Intervals shown were chosen to represent the timing of fast-ice formation (May–July) and breakout (September–November) at the South Orkney Islands, and the time of maximum lagged correlations of SOFI with ENSO (Jun-Aug of the previous year). Stars in plots (b and g) denote the location of the South Orkney Islands.

5.2. Regional Connections and Influences of ENSO and SAM-Related Processes on Weddell Sea-Ice

Our results are consistent with the emerging understanding of the atmospheric and oceanic influences on sea-ice in the region. Changes in SIE and concentration in the western Weddell Sea have been linked to the influence of ENSO and SAM modes of climate variability [*Stammerjohn et al*., 2008b; *McKee et al*., 2011; *Pezza et al*., 2008, 2012]. The ASL is the dominant regional influence on atmospheric circulation and ocean and sea-ice dynamics in Amundsen-Bellingshausen Sea and western Weddell Sea [e.g., *Liu et al*., 2004; *Turner et al*., 2013]. ENSO and SAM modes influence the depth and location of the ASL, which is deeper during La Niña events and when SAM polarity is positive, although the relationships vary seasonally [*Fogt et al*., 2011; *Simpkins et al*., 2012; *Clem and Fogt*, 2013; *Turner et al*., 2013]. Previous work has found that SIE in the western Weddell Sea is increased when southerly winds are increased in association with negative SAM polarity and warm El Niño events [*Stammerjohn et al*., 2008b; *Fogt et al*., 2011; *McKee et al*., 2011; *Pezza et al*., 2008, 2012; *Simpkins et al*., 2012]. As we have shown, South Orkney fast-ice duration and Weddell SIE and concentration are correlated, and are a function of both the timing of advance of sea-ice in autumn and retreat in

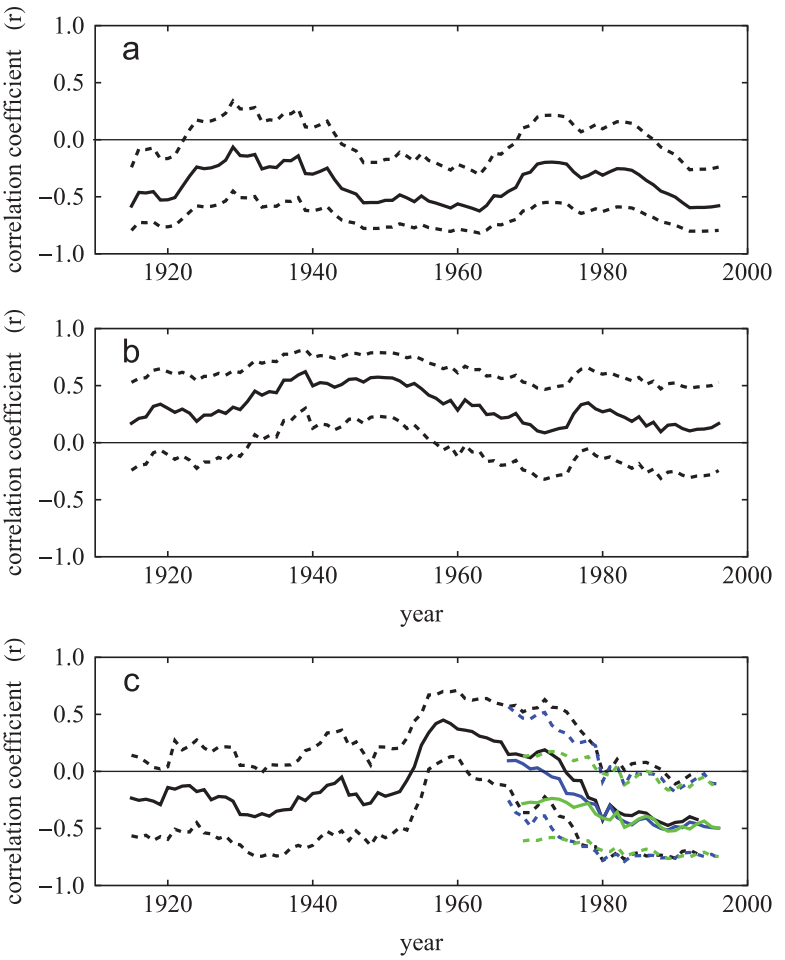

Figure 12. Moving 25 year correlations between (a) sea-ice formation and (b) breakout and NINO3.4 SST anomalies in June–August of the previous year, and (c) breakout with the mean SAM index for September, October, and November (SON; extended SAM index) [*Fogt et al.*, 2009]. Black solid lines show *r* values and dashed lines give 95% confidence interval. For comparison, the blue lines show the correlation (±95% CI) of breakout with the mean SON values of the *Marshall* [2003] SAM index and the green lines show the correlation for just September.

spring [see also *Murphy et al.*, 1995]. Our results show that fast-ice formation (and hence sea-ice advance), and also fast-ice breakout (and likewise sea-ice retreat), are influenced in different ways by changes in the ASL region and variation in ENSO and SAM.

During spring, the variability in timing of the sea-ice retreat and the subsequent fast-ice breakout is associated with variations in atmospheric conditions. Stronger westerlies in the Drake Passage region are associated with the intensification of the ASL to the west of the Antarctic Peninsula associated with a positive SAM polarity and a cold ENSO (La Niña) phase in the tropical Pacific [*Stammerjohn et al.*, 2008b; *Turner et al.*, 2013]. The deepening of the ASL generates a north-westerly component to the air-flow in the region of the South Orkney Islands (Figure 7b), resulting in warmer air from the southern Pacific being brought into the northern Weddell Sea region [see also *Thompson and Solomon*, 2002]. This also results in the Atlantic Sector being unusual in its SST response to stronger westerly winds (positive SAM) compared to the rest of the Southern Ocean, with SSTs anomalously warm across the Scotia Sea when the SAM is positive [*Meredith et al.*, 2008]. Studies using general ocean circulation models also indicate that the northward component of the surface current velocities is reduced around the tip of the Peninsula during these positive SAM/La Niña periods [*Renner et al.*, 2012]. This combination of oceanic and atmospheric conditions will reduce northward motion, potentially blocking advance of sea-ice into the Scotia Sea, and with warmer air and sea temperatures there will be an increased melt and earlier southward retreat of ice during spring (and in turn reducing the winter northward ice extent and duration) and also earlier breakout of fast-ice. When the SAM is

negative during a warm El Niño phase, MSLP is high to the west of the Antarctic Peninsula, and meridional winds in the western Weddell Sea are stronger (Figure 7a), resulting in earlier advance in autumn and increased advection of sea-ice northward and cooler atmospheric and oceanic conditions. The processes involved are interactive, but our findings suggest that in recent decades the atmospheric variation associated with SAM has played a greater role in processes of fast-ice breakout and sea-ice retreat during spring. Variation associated with ENSO has had a greater influence on processes of fast-ice formation and autumn sea-ice advance in the western Weddell Sea, which are also affected by propagating anomalies in oceanic and ice conditions.

Through the extended fast-ice series, we observe temporal changes in the variability of fast-ice formation and breakout. We also observe temporal changes in the correlation strength with ENSO and SAM, which may reflect natural internal variability associated with both modes [*Divine et al*., 2009; *McKee et al*., 2011]. The changing frequencies of variability in formation and breakout may therefore be associated with the variable interactive regional and local impacts of changing ENSO phases and polarity of SAM. The sea-ice dynamics in the northern Weddell Sea region are dependent on the instantaneous interaction of atmospheric variability associated with ENSO and SAM [*Stammerjohn et al*., 2008b; *Fogt et al*., 2011; *Simpkins et al*., 2012; *Turner et al*., 2013] and also on the propagating oceanic/ice anomalies in the Pacific and Weddell Sea region that are themselves also affected by ENSO and SAM variability. At times (e.g., between 1965 and 1994) the spatial and temporal coherence of anomalies of the SST and ice series at the circumpolar scale has been particularly strong [*Murphy et al*., 1995; *White and Peterson*, 1996], but this is a variable feature [*Venegas et al*., 2001]. This period was associated with increasingly positive SAM, and hence increased intensity of the westerlies winds, which may increase eastward drift of anomalies in sea-ice and SST in the Southern Pacific [*Meredith et al*., 2008]. The potential for feedback effects from the ice and ocean variability to reinforce or dampen atmospheric variation has been noted [*Venegas and Drinkwater*, 2001; *Raphael et al*., 2011], and is likely to be a key aspect of the Bellingshausen/Weddell Sea variation, which encompasses much of the region of high sea-ice variability in the Southern Ocean [*McKee et al*., 2011; *Pezza et al*., 2012].

5.3. Long-Term Changes in Timing of Fast-Ice Formation and Breakout

A key feature of the SOFI series is the reduction in mean duration between ~1945 and 1965, consistent with the earlier analyses of the shorter time series [*Murphy et al*., 1995]. The updated series and analyses including the formation and breakout dates show that the change in duration reflected a significant trend of later formation of fast-ice, but that the linear trend in breakout date was not significant. The wavelet analysis indicates that the major change in duration reflected decadal changes in the timing of fast-ice formation and breakout. This occurred during the period of overlap of the two series and both sites recorded a change in fast-ice duration. The strongest evidence that a change occurred comes from the single Scotia Bay series which ran until 1975 and is therefore unaffected by the change in sampling methods and locations that affects the full SOFI series. The wavelet analysis for the Scotia Bay series indicated that the variation in both series was similar during the overlap period. The sequential detection analysis also demonstrates that the SOFI series has maintained the same major feature of the Scotia Bay series with a change in mean duration and breakout detected at ~1951. While the major features of fast-ice variability are consistent across the different series, the change in observation location may have a small influence on the analysis of trends due to differing methods that could be employed to join the two data sets into a continuous fast-ice record.

There are very few data available to validate the observed change in duration or to assess the scale of such a change although some analyses have been undertaken. Historical ship charts from whaling in Antarctic waters indicate a reduction in Southern Ocean SIE during the period from the 1940s to the 1960s [*de la Mare*, 1997], although see also the discussion in *Ackley et al*. [2003]. Further regional analysis of whaling charts and other historical information indicated that 20th century sea-ice declines were particularly strong in the Weddell Sea region, and suggestive of a greater winter SIE with decreased seasonal change during the early part of the 20th century [*Cotte and Guinet*, 2007; *de la Mare*, 2009].

The concentration of methaneosulfonic acid (MSA) in ice cores has been proposed as a proxy for winter SIE, because it is derived from biological productivity in the marginal sea-ice zone during the spring sea-ice retreat [see, e.g., *Welch et al*., 1993; *Curran et al*., 2003; *Abram et al*., 2013]. Positive correlations were found between satellite sea-ice records and MSA at Law Dome over the period from 1973 to 1995 [*Curran et al*.,

2003]. The sea-ice reconstruction extended back to 1841 and suggested that winter SIE in the Law Dome region had decreased by around 20% since the 1950s [*Curran et al*., 2003]. Ice cores from the western Antarctic Peninsula indicate a progressive sea-ice decline in the Bellingshausen Sea region throughout the 20th century, and which has been fastest since ~1958 [*Abram et al*., 2010, 2013]. Comparison of these regional sea-ice reconstructions with the SOFI series suggests that, while each region has experienced a long-term decrease in sea-ice during the 20th century, the timing of these changes has varied markedly. These regional differences are not surprising as satellite observations show that since 1979 the sea-ice trends in these regions have not been uniform [*Turner et al*., 2009].

It is notable that the change in fast-ice duration was also associated with the onset of regional warming around the South Orkney Islands where air temperatures have increased by over 1°C after about 1950 [*Zazulie et al*., 2010]. However, since that time there was no trend in the SOFI series while air temperatures have continued to increase [*Zazulie et al*., 2010]. The midcentury change in fast-ice formation and breakout was also associated with a period when variations in both series were correlated with ENSO, but the correlation with breakout decreased after that time, while the correlation with SAM increased from 1957 (when the *Marshal* [2003] SAM series began; Figure 12). This raises the possibility of a link to changes in SST of the tropical Pacific. Decadal-variability recorded in ice-cores influenced by climate in the Amundsen Sea region have been attributed to long-time scale SST variability originating in the tropical Pacific region [*Ding et al*., 2011; *Steig et al*., 2013]. The role of extratropical forcing in driving secular changes in Antarctic sea-ice clearly warrants further study.

Analyses of satellite sea-ice data have found that advance and retreat dates have changed across the northwestern Weddell Sea region since 1979 [*Stammerjohn et al*., 2008b]. However, these are not significant in the South Orkney area and there are no statistically significant trends in any of the SOFI series during the last 30 years. The changing dominant frequencies of variability in the formation and breakout series over the last century, suggested that trends in Weddell Sea region sea-ice based on the relatively shorter-term satellite data should be treated with caution. Future projections of sea-ice change in regions of the Southern Ocean are highly uncertain. It has been suggested the increasingly positive trend in SAM in summer is related to the depletion of ozone, and that future greenhouse gas increases are expected to cause positive trends in winter SAM over the coming century and a projected one third reduction in sea-ice by 2100 [*Bracegirdle et al*., 2008; *Turner et al*., 2009; *Thompson et al*., 2011]. The positive trends in the SAM would be expected to generate earlier breakouts of fast-ice at the South Orkneys and reduced ice durations and extents across the Scotia Sea.

6. Conclusions and Summary

Comparisons with satellite data (post-1979) show that the fast-ice series at the South Orkney Islands is representative of the seasonal variability of sea-ice across a wider area of the northern Weddell and Scotia Sea. The date of ice breakout is associated with the timing of retreat of sea-ice across the Scotia Sea and influenced by wind strength and direction during spring. More intense westerly/north-westerley winds occur when SAM is positive and are associated with earlier breakout of fast-ice. Fast-ice formation is influenced by local and regional conditions during autumn, but is also dependent on long-term conditions over the previous 1–2 years in both the Weddell Sea and Amundsen-Bellingshausen Sea regions. These variations are associated with the propagation of anomalies across this region of the Southern Ocean as well as variations in ENSO. These different impacts of atmospheric processes and variability on the formation and breakout of fast-ice, and the wider regional sea-ice dynamics, emphasize the need for resolution of seasonal processes in understanding changes in winter sea-ice extent around Antarctica.

The formation and breakout of fast-ice at the South Orkney Islands has shown marked interannual variability and longer term changes over the last century. There does appear to have been a change in the fast-ice duration between the 1940s and 1960s as a result of later ice formation and earlier ice breakout. This was associated with the start of the period of increasing regional air temperatures, however, fast-ice has not shown a simple linear decline with increasing temperatures over the last 50 years. Overall, there is little evidence of a decline in sea-ice in this region over the last 30–50 years, with the dynamics instead being dominated by changing frequencies of variability. Changes in fast-ice variability are also associated with nonstationary relationships with ENSO and SAM, which further emphasizes that analyses of sea-ice change based only on a few decades of data should be interpreted with caution.

Acknowledgments
We thank the members of BAS and other scientists who have supported and maintained the fast-ice data collection. We would like to thank three anonymous referees for their comments, which greatly improved the manuscript. The study was supported through the BAS Polar Science for Planet Earth Programme funded by the Natural Environment Research Council, UK. N.J.A. is supported by a Queen Elizabeth II fellowship awarded by the Australian Research Council (DP110101161). This study was aided by the use of the KNMI Climate Explorer web resource provided by G. J. van Oldenborgh. J. Forcada is gratefully acknowledged for advice and undertaking the multivariate time series analyses, T. Phillips for processing the ERA-INTERIM data and preparation of selected figures, J. Wilkinson for discussion of the controls on fast-ice, and P. Fretwell for producing the map figure. The SOFI series data shown in Figure 2 are available through the BAS Polar Data Centre, http://dx.doi.org/tqw.

References

Abram, N. J., R. Mulvaney, E. W. Wolff, and M. Mudelsee (2007), Ice core records as sea ice proxies: An evaluation from the Weddell Sea region of Antarctica, *J. Geophys. Res.*, *112*, D15101, doi:10.1029/2006JD008139.

Abram, N. J., E. R. Thomas, J. R. McConnell, R. Mulvaney, T. J. Bracegirdle, L. C. Sime, and A. J. Aristarain (2010), Ice core evidence for a 20th century decline of sea ice in the Bellingshausen Sea, Antarctica, *J. Geophys. Res.*, *115*, D23101, doi:10.1029/2010JD014644.

Abram, N. J., E. W. Wolff, and M. A. J. Curran (2013), A review of sea ice proxy information from polar ice cores, *Quat. Sci. Rev.*, *79*, 168–183, doi:10.1016/j.quascirev.2013.01.011.

Ackley, S., P. Wadhams, J. C. Comiso, and A. P. Worby (2003), Decadal decrease of Antarctic sea ice extent inferred from whaling records revisited on the basis of historical and modern sea ice records, *Polar Res.*, *22*(1), 19–25.

Bracegirdle, T. J., W. M. Connolley, and J. Turner (2008), Antarctic climate change over the Twenty First Century, *J. Geophys. Res.*, *113*, D03103, doi:10.1029/2007JD008933.

Brierley, A. S., and D. N. Thomas (2002), Ecology of Southern Ocean pack ice, *Adv. Mar. Biol.*, *43*, 171–276, doi:10.1016/S0065-2881(02)43005-2.

Burnham, K. P., and D. R. Anderson (2002), *Model Selection and Multimodel Inference: A Practical Information-Theoretic Approach*, 2nd ed., vol. XXVI, 488 pp., Springer, N. Y.

Cavalieri, D. J., and C. L. Parkinson (2008), Antarctic sea ice variability and trends, *1979–2006. J. Geophys. Res.*, *113*, C07004, doi:10.1029/2007JC004564.

Clarke, A., E. J. Murphy, M. P. Meredith, J. C. King, L. S. Peck, D. K. A. Barnes, and R. C. Smith (2007), Climate change and the marine ecosystem of the western Antarctic Peninsula, *Philos. Trans. R. Soc. B*, *362*, 149–166, doi:10.1098/rstb.2006.1958.

Clem, K. R., and R. L. Fogt (2013), Varying roles of ENSO and SAM on the Antarctic Peninsula climate in austral spring, *J. Geophys. Res.*, *118*, 11,481–11,492, doi:10.1002/jgrd.50860.

Cole, J. E., R. G. Fairbanks, and G. T. Shen (1993), Recent variability in the Southern Oscillation—Isotopic results from a Tarawa Atoll coral, *Science*, *260*(5115), 1790–1793, doi:10.1126/science.260.5115.1790.

Comiso, J. C., and F. Nishio (2008), Trends in the sea ice cover using enhanced and compatible AMSR-E, SSM/I, and SMMR data, *J. Geophys. Res.*, *113*, C02S07, doi:10.1029/2007JC004257.

Cotte, C., and C. Guinet (2007), Historical whaling records reveal major regional retreat of Antarctic sea ice, *Deep Sea Res., Part I*, *54*, 243–252, doi:10.1016/j.dsr.2006.11.001.

Crocker, G. B., and P. Wadhams (1989), Breakup of Antarctic fast ice, *Cold Reg. Sci. Technol.*, *17*, 61–76, doi:10.1016/S0165-232X(89)80016-3.

Curran, M. A. J., T. D. van Ommen, V. I. Morgan, K. L. Phillips, and A. S. Palmer (2003), Ice core evidence for Antarctic sea ice decline since the 1950s, *Science*, *302*(5648), 1203–1206, doi:10.1126/science.1087888.

de la Mare, W. K. (1997), Abrupt mid-twentieth-century decline in Antarctic sea-ice extent from whaling records, *Nature*, *389*(6646), 57–60, doi:10.1038/37956.

de la Mare, W. K. (2009), Changes in Antarctic sea-ice extent from direct historical observations and whaling records, *Clim. Change*, *92*(3–4), 461–493, doi:10.1007/s10584-008-9473-2.

Dee, D. P., et al. (2011), The ERA-Interim reanalysis: Configuration and performance of the data assimilation system, *Q. J. R. Meteorol. Soc.*, *137*, 553–597, doi:10.1002/qj.828.

Ding, Q., E. J. Steig, D. S. Battisti, and M. Kuttel (2011), Winter warming in West Antarctica caused by central tropical Pacific warming, *Nat. Geosci.*, *4*(6), 398–403, doi:10.1038/ngeo1129.

Divine, D. V., E. Isaksson, M. Kaczmarska, F. Godtliebsen, H. Oerter, E. Schlosser, S. J. Johnsen, M. van den Broeke, and R. S. W. van de Wal (2009), Tropical Pacific-high latitude south Atlantic teleconnections as seen in delta O-18 variability in Antarctic coastal ice cores, *J. Geophys. Res.*, *114*, D11112, doi:10.1029/2008JD010475.

Ducklow, H. W., K. Baker, D. G. Martinson, L. B. Quetin, R. M. Ross, R. C. Smith, S. E. Stammerjohn, M. Vernet, and W. Fraser (2007), Marine pelagic ecosystems: The West Antarctic Peninsula, *Philos. Trans. R. Soc. B*, *362*(1477), 67–94, doi:10.1098/rstb.2006.1955.

Fogt, R. L., J. Perlwitz, A. J. Monaghan, D. H. Bromwich, J. M. Jones, and G. J. Marshall (2009), Historical SAM variability. Part II: Twentieth-century variability and trends from reconstructions, observations, and the IPCC AR4 models, *J. Clim.*, *22*, 5346–5365, doi:10.1175/2009JCLI2786.1.

Fogt, R. L., D. H. Bromwich, and K. M. Hines (2011), Understanding the SAM influence on the South Pacific ENSO teleconnection, *Clim. Dyn.*, *36*, 1555–1576, doi:10.1007/s00382-010-0905-0.

Fraser, A. D., R. A. Massom, K. J. Michael, B. K. Galton-Fenzi, and J. L. Lieser (2012), East Antarctic landfast sea ice distribution and variability, 2000–08, *J. Clim.*, *25*, 1137–1156, doi:10.1175/JCLI-D-10-05032.1.

Fretwell, P. T., P. N. Trathan, B. Wienecke, and G. L. Kooyman (2014), Emperor penguins breeding on iceshelves, *PLoS One 9*(1), e85285, doi:10.1371/journal.pone.0085285.

Hartmann, D. L., and F. Lo (1998), Wave-driven zonal flow vacillation in the Southern Hemisphere, *J. Atmos. Sci.*, *55*, 1303–1315, doi:10.1175/1520-0469(1998)055<1303:WDZFVI>2.0.CO;2.

Hobbs, W. R., and M. N. Raphael (2010), The Pacific zonal asymmetry and its influence on Southern Hemisphere sea ice variability, *Antarct. Sci.*, *22*(5), 559–571, doi:10.1017/S0954102010000283.

Holland, M. M., and M. N. Raphael (2006), Twentieth century simulation of the southern hemisphere climate in coupled models. Part II: Sea ice conditions and variability, *Clim. Dyn.*, *26*(2–3), 229–245, doi:10.1007/s00382-005-0087-3.

Holland, P., and R. Kwok (2012), Wind-driven trends in Antarctic sea-ice drift, *Nat. Geosci.*, *5*, 872–875, doi:10.1038/ngeo1627.

Kaplan, A., M. A. Cane, Y. Kushnir, A. C. Clement, M. B. Blumenthal, and B. Rajagopalan (1998), Analyses of global sea surface temperature 1856–1991, *J. Geophys. Res.*, *103*, 18567–18589, doi:10.1029/97JC01736.

Kravchenko, V. O., O. M. Evtushevsky, A. V. Grytsai, and G. P. Milinevsky (2011), Decadal variability of winter temperatures in the Antarctic Peninsula region, *Antarct. Sci.*, *23*(6), 614–622, doi:10.1017/S0954102011000423.

Lefebvre, W., and H. Goosse (2008), An analysis of the atmospheric processes driving the large-scale winter sea ice variability in the Southern Ocean, *J. Geophys. Res.*, *113*, C02004, doi:10.1029/2006JC004032.

Liu, J. P., J. A. Curry, and D. G. Martinson (2004), Interpretation of recent Antarctic sea ice variability, *Geophys. Res. Lett.*, *31*, L02205, doi:10.1029/2003GL01873.

Mahoney, A., H. Eicken, A. G. Gaylord, and L. Shapiro (2007a), Alaska landfast sea ice: Links with bathymetry and atmospheric circulation, *J. Geophys. Res.*, *112*, C02001, doi:10.1029/2006JC003559.

Mahoney, A., H. Eicken, and L. Shapiro (2007b), How fast is landfast sea ice? A study of the attachment and detachment of nearshore ice at Barrow, Alaska, *Cold Reg. Sci. Technol.*, *47*, 233–255, doi:10.1016/j.coldregions.2006.09.005.

Marshall, G. J. (2003), Trends in the southern annular mode from observations and reanalyses, *J. Clim.*, *16*(24), 4134–4143, doi:10.1175/1520-0442(2003)016<4134:TITSAM>2.0.CO;2.

Marshall, G. J., S. Di Battista, S. S. Naik, and M. Thamban (2011), Analysis of a regional change in the sign of the SAM-temperature relationship in Antarctica, *Clim. Dyn.*, *36*(1–2), 277–287, doi:10.1007/s00382-009-0682-9.

Massom, R. A., K. Hill, C. Barbraud, N. Adams, A. Ancel, L. Emmerson, and M. J. Pook (2009), Fast ice distribution in Adelie Land, East Antarctica: Interannual variability and implications for emperor penguins *Aptenodytes forsteri*, *Mar. Ecol. Prog. Ser.*, *374*, 243–257, doi:10.3354/meps07734.

Massom, R. A., A. B. Giles, H. A. Fricker, R. C. Warner, B. Legresy, G. Hyland, N. Young, and A. D. Fraser (2010), Examining the interaction between multi-year landfast sea ice and the Mertz Glacier Tongue, East Antarctica: Another factor in ice sheet stability?, *J. Geophys. Res.*, *115*, C12027, doi:10.1029/2009JC006083.

McKee, D. C., X. Yuan, A. L. Gordon, B. A. Huber, and Z. Dong (2011), Climate impact on interannual variability of Weddell Sea Bottom Water, *J. Geophys. Res.*, *116*, C05020, doi:10.1029/2010JC006484.

Melbourne-Thomas, J., A. Constable, S. Wotherspoon, and B. Raymond (2013), Testing paradigms of ecosystem change under climate warming in Antarctica, *PLoS ONE*, *8*(2), e55093, doi:10.1371/journal.pone.0055093.

Meredith, M. P., E. J. Murphy, E. J. Hawker, J. C. King, and M. I. Wallace (2008), On the interannual variability of ocean temperatures around South Georgia, Southern Ocean: Forcing by El Niño/Southern Oscillation and the Southern Annular Mode, *Deep Sea Res., Part II*, *55*(18–19), 2007–2022, doi:10.1016/j.dsr2.2008.05.020.

Murphy, E. J., A. Clarke, C. Symon, and J. Priddle (1995), Temporal variation in Antarctic sea-ice—Analysis of a long-term fast-ice record from the South-Orkney Islands, *Deep Sea Res., Part I*, *42*(7), 1045–1062, doi:10.1016/0967-0637(95)00057-D.

Murphy, E. J., P. N. Trathan, J. L. Watkins, K. Reid, M. P. Meredith, J. Forcada, S. E. Thorpe, N. M. Johnston, and P. Rothery (2007a), Climatically driven fluctuations in Southern Ocean ecosystems, *Proc. R. Soc. B*, *274*(1629), 3057–3067, doi:10.1098/rspb.2007.1180.

Murphy, E. J., et al. (2007b), Spatial and temporal operation of the Scotia Sea ecosystem: A review of large-scale links in a krill centred food web, *Philos. Trans. R. Soc. B*, *362*(1477), 113–148, doi:10.1098/rstb.2006.1957.

Nicol, S., A. Worby, and R. Leaper (2008), Changes in the Antarctic sea ice ecosystem: Potential effects on krill and baleen whales, *Mar. Freshwater Res.*, *59*, 361–382, doi:10.1071/MF07161.

Petrich, C., H. Eicken, J. Zhang, J. Krieger, Y. Fukamachi, and K. I. Ohshima (2012), Coastal landfast sea ice decay and breakup in northern Alaska: Key processes and seasonal prediction, *J. Geophys. Res.*, *117*, C02003, doi:10.1029/2011JC007339.

Pezza, A. B., T. Durrant, I. Simmonds, and I. Smith (2008), Southern hemisphere synoptic behavior in extreme phases of SAM, ENSO, sea ice extent, and Southern Australia Rainfall, *J. Clim.*, *21*(21), 5566–5584, doi:10.1175/2008JCLI2128.1.

Pezza, A. B., H. A. Rashid, and I. Simmonds (2012), Climate links and recent extremes in antarctic sea ice, high-latitude cyclones, Southern Annular Mode and ENSO, *Clim. Dyn.*, *38*(1–2), 57–73, doi:10.1007/s00382-011-1044-y.

Raphael, M. N., W. Hobbs, and I. Wainer (2011), The effect of Antarctic sea ice on the Southern Hemisphere atmosphere during the southern summer, *Clim. Dyn.*, *36*(7–8), 1403–1417, doi:10.1007/s00382-010-0892-1.

Reiss, C. S., C. D. Hewes, and O. Holm-Hansen (2009), Influence of atmospheric teleconnections and Upper Circumpolar Deep Water on phytoplankton biomass around Elephant Island, Antarctica, *Mar. Ecol. Prog. Ser.*, *377*, 51–62, doi:10.3354/meps07840.

Renner, A. H. H., S. E. Thorpe, K. J. Heywood, E. J. Murphy, J. L. Watkins, and M. P. Meredith (2012), Advective pathways near the tip of the Antarctic Peninsula: Trends, variability and ecosystem implications, *Deep Sea Res., Part I*, *63*, 91–101, doi:10.1016/j.dsr.2012.01.009.

Reynolds, R. W., N. A. Rayner, T. M. Smith, D. C. Stokes, and W. Wang (2002), An improved in situ and satellite SST analysis for climate, *J. Clim.*, *15*, 1609–1625, doi:10.1175/1520-0442(2002)015<1609:AIISAS>2.0.CO;2.

Rodionov, S. N. (2004), A sequential algorithm for testing climate regime shifts, *Geophys. Res. Lett.*, *31*, L09204, doi:10.1029/2004GL019448.

Rodionov, S. N. (2006), Use of prewhitening in climate regime shift detection, *Geophys. Res. Lett.*, *33*, L12707, doi:10.1029/2006GL025904.

Simpkins, G. R., L. M. Ciasto, D. W. J. Thompson, and M. H. England (2012), Seasonal relationships between large-scale climate variability and Antarctic Sea Ice concentration, *J. Clim.*, *25*(16), 5451–5469, doi:10.1175/JCLI-D-11-00367.1.

Squire, V. A. (1993), The breakup of fast shore ice, *Cold Reg. Sci. Technol.*, *21*, 211–218, doi:10.1016/0165-232X(93)90065-G.

Stammerjohn, S. E., D. G. Martinson, R. C. Smith, and R. A. Iannuzzi (2008a), Sea ice in the western Antarctic Peninsula region: Spatio-temporal variability from ecological and climate change perspectives, *Deep Sea Res., Part II*, *55*(18–19), 2041–2058, doi:10.1016/j.dsr2.2008.04.026.

Stammerjohn, S. E., D. G. Martinson, R. C. Smith, X. Yuan, and D. Rind (2008b), Trends in Antarctic annual sea ice retreat and advance and their relation to El Niño-Southern Oscillation and Southern Annular Mode variability, *J. Geophys. Res.*, *113*, C03S90, doi:10.1029/2007JC004269.

Steig, E. J., et al. (2013), Recent climate and ice-sheet changes in West Antarctica compared with the past 2,000 years, *Nat. Geosci.*, *6*(5), 372–375, doi:10.1038/ngeo1778.

Thompson, D. W. J., and S. Solomon (2002), Interpretation of recent Southern Hemisphere climate change, *Science*, *296*, 895–899, doi:10.1126/science.1069270.

Thompson, D. W. J., and J. M. Wallace (2000), Annular modes in the extratropical circulation. Part I: Month-to-month variability, *J. Clim.*, *13*(5), 1000–1016, doi:10.1175/1520-0442(2000)013<1000:AMITEC>2.0.CO;2.

Thompson, D. W. J., S. Solomon, P. J. Kushner, M. H. England, K. M. Grise, and D. J. Karoly (2011), Signatures of the Antarctic ozone hole in Southern Hemisphere surface climate change, *Nat. Geosci.*, *4*(11), 741–749, doi:10.1038/ngeo1296.

Torrence, C., and G. P. Compo (1998), A practical guide to wavelet analysis, *Bull. Am. Meteorol. Soc.*, *79*, 61–78, doi:10.1175/1520-0477.

Turner, J. (2004), The El Niño Southern Oscillation and Antarctica, *Int. J. Climatol.*, *24*(1), 1–31, doi:10.1002/joc.965.

Turner, J., and J. Overland (2009), Contrasting climate change in the two polar regions, *Polar Res.*, *28*(2), 146–164, doi:10.1111/j.1751-8369.2009.00128.x.

Turner, J., J. C. Comiso, G. J. Marshall, T. A. Lachlan-Cope, T. Bracegirdle, T. Maksym, M. P. Meredith, Z. M. Wang, and A. Orr (2009), Non-annular atmospheric circulation change induced by stratospheric ozone depletion and its role in the recent increase of Antarctic sea ice extent, *Geophys. Res. Lett.*, *36*, L08502, doi:10.1029/2009GL037524.

Turner, J., T. Maksym, T. Phillips, G. J. Marshall, and M. P. Meredith (2012), The impact of changes in sea ice advance on the large winter warming on the western Antarctic Peninsula, *Int. J. Climatol.*, *33*(4), 852–861, doi:10.1002/joc.3474.

Turner, J., T. Phillips, J. S. Hosking, G. J. Marshall, and A. Orr (2013), The Amundsen Sea Low, *Int. J. Climatol.*, *33*(7), 1818–1829, doi:10.1002/joc.3558.

Urban, F. E., J. E. Cole, and J. T. Overpeck (2000), Influence of mean climate change on climate variability from a 155-year tropical Pacific coral record, *Nature*, *407*(6807), 989–993, doi:10.1038/35039597.

Venegas, S. A., and M. R. Drinkwater (2001), Sea ice, atmosphere and upper ocean variability in the Weddell Sea, Antarctica, *J. Geophys. Res.*, *106*, 16,747–16,765, doi:10.1029/2000JC000594.

Venegas, S. A., M. R. Drinkwater, and G. Shaffer (2001), Coupled oscillations in Antarctic sea ice and atmosphere in the South Pacific sector, *Geophys. Res. Lett.*, *28*, 3301–3304, doi:10.1029/2001GL012991.

Welch, K. A., P. A. Mayewski, and S. I. Whitlow (1993), Methanesulfonic-acid in coastal Antarctic snow related to sea-ice extent, *Geophys. Res. Lett.*, *20*, 443–446, doi:10.1029/93GL00499.

White, W. B., and R. G. Peterson (1996), An Antarctic circumpolar wave in surface pressure, wind, temperature and sea-ice extent, *Nature*, *380*(6576), 699–702, doi:10.1038/380699a0.

WMO (World Meterological Organisation) (1970), The WMP sea-ice nomeclature. Terminology, codes and illustrated glossary, *WMO/OMM/BMO 259, TP 145*, World Meterol. Organ., Geneva.

Wu, Q., and X. Zhang (2011), Observed evidence of an impact of the Antarctic sea ice dipole on the Antarctic oscillation, *J. Clim.*, *24*(16), 4508–4518, doi:10.1175/2011JCLI3965.1.

Yuan, X., and C. Li (2008), Climate modes in southern high latitudes and their impacts on Antarctic sea ice, *J. Geophys. Res.*, *113*, C06S91, doi:10.1029/2006JC004067.

Yuan, X. J., and D. G. Martinson (2000), Antarctic sea ice extent variability and its global connectivity, *J. Clim.*, *13*(10), 1697–1717.

Zazulie, N., M. Rusticucci, and S. Solomon (2010), Changes in climate at high southern altitudes: A unique daily record at Orcadas spanning 1903–2008, *J. Clim.*, *23*, 189–196, doi:10.1175/2009JCLI3074.1.

Zwally, H. J., J. C. Comiso, C. L. Parkinson, D. J. Cavalieri, and P. Gloersen (2002), Variability of Antarctic sea ice 1979–1998, *J. Geophy. Res.*, *107*, 9-1–9-21, doi:10.1029/2000JC000733.